AD-A166 293 STUDY OF TEST METHODS FOR URETHANE ELASTOMERS(U) 1/1
SOUTHWEST RESEARCH INST SAN ANTONIO TX DIV OF
ENGINEERING AND MATERIALS SCIENCE J J DZIUK ET AL.
UNCLASSIFIED 18 OCT 85 BFLRF-204 DAAK70-85-C-0007 F/G 11/10 NL

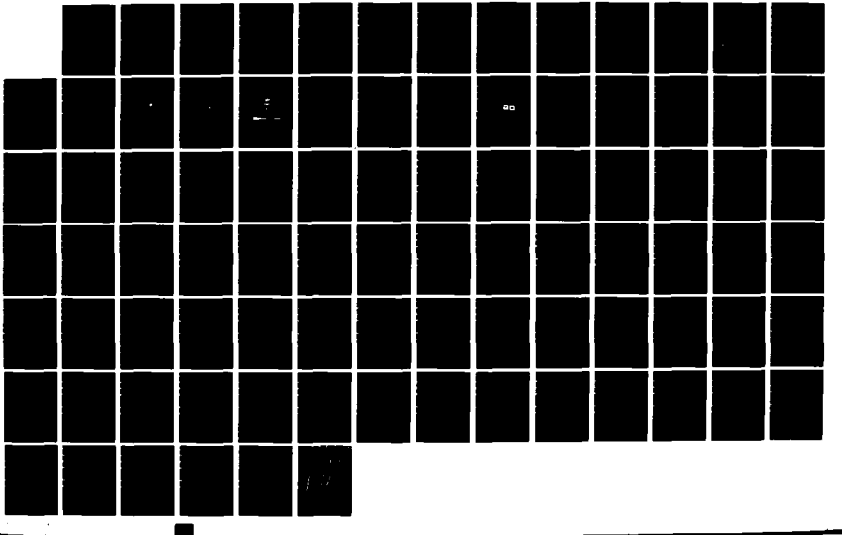

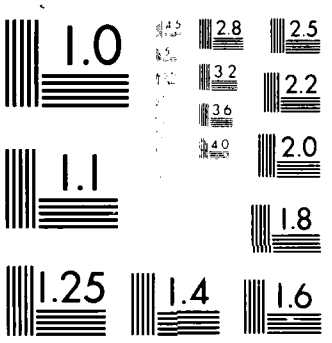

STUDY OF TEST METHODS FOR URETHANE ELASTOMERS

INTERIM REPORT
BFLRF No. 204

By

J.J. Dziuk, Jr.
W.A. McMahon
C.H. Parr
W.A. Mallow
H.S. Silvus
Engineering and Materials Sciences Division
Southwest Research Institute
San Antonio, Texas

Prepared for

Belvoir Fuels and Lubricants Research Facility (SwRI)
Southwest Research Institute
San Antonio, Texas

Under Contract to

U.S. Army Belvoir Research
and Development Center
Materials, Fuels and Lubricants Laboratory
Fort Belvoir, Virginia

Contract No. DAAK70-85-C-0007

October 1985

UNCLASSIFIED
SECURITY CLASSIFICATION OF THIS PAGE

AD-A166 193

REPORT DOCUMENTATION PAGE

1a. REPORT SECURITY CLASSIFICATION Unclassified	1b. RESTRICTIVE MARKINGS None
2a. SECURITY CLASSIFICATION AUTHORITY N/A	3. DISTRIBUTION/AVAILABILITY OF REPORT Approved for public release; distribution unlimited
2b. DECLASSIFICATION/DOWNGRADING SCHEDULE	
4. PERFORMING ORGANIZATION REPORT NUMBER(S) Interim Report BFLRF No. 204	5. MONITORING ORGANIZATION REPORT NUMBER(S)
6a. NAME OF PERFORMING ORGANIZATION Southwest Research Institute Engineering & Materials Sciences Division 6b. OFFICE SYMBOL (If applicable)	7a. NAME OF MONITORING ORGANIZATION
6c. ADDRESS (City, State, and ZIP Code) 6220 Culebra Road San Antonio, TX 78284	7b. ADDRESS (City, State, and ZIP Code)
8a. NAME OF FUNDING/SPONSORING ORGANIZATION Belvoir Research, Development and Engineering Center 8b. OFFICE SYMBOL (If applicable) STRBE-VF	9. PROCUREMENT INSTRUMENT IDENTIFICATION NUMBER DAAK70-85-C-0007, WD 26
8c. ADDRESS (City, State, and ZIP Code) Ft. Belvoir, VA 22060-5606	10. SOURCE OF FUNDING NUMBERS PROGRAM ELEMENT NO. / PROJECT NO. / TASK NO. / WORK UNIT ACCESSION NO.

11. TITLE (Include Security Classification)

Study of Test Methods for Urethane Elastomers (U)

12. PERSONAL AUTHOR(S)
Dziuk, Jr., J.J.; McMahon, W.A.; Parr, C.H.; Mallow, W.A.; and Silvus, H.S.

13a. TYPE OF REPORT	13b. TIME COVERED	14. DATE OF REPORT (Year, Month, Day)	15. PAGE COUNT
Interim	FROM Apr. 85 TO Sept. 85	1985 October 18	83

16. SUPPLEMENTARY NOTATION
This work was performed under a contract issued to the Belvoir Fuels and Lubricants Research Facility (SwRI) by the U.S. Army Belvoir RD&E Center, Ft. Belvoir, VA 22060-5606.

17. COSATI CODES			18. SUBJECT TERMS (Continue on reverse if necessary and identify by block number)
FIELD	GROUP	SUB-GROUP	Polyurethane Fuel Tank Resistivity

19. ABSTRACT (Continue on reverse if necessary and identify by block number)

The feasibility of using a portable instrument to determine the physical condition of fabric-reinforced polyurethane fuel tanks was studied during this project. The condition of the polyurethane was determined by measuring its surface electrical resistivity. Electrical resistivity of a polymer will change as it ages or deteriorates. An instrument designed and built by Southwest Research Institute personnel was found to be effective in determining the relative surface resistivity of polyurethane. This instrument was able to measure the surface resistivity of polyurethane samples in varying degrees of degradation due to humid aging.

20. DISTRIBUTION/AVAILABILITY OF ABSTRACT	21. ABSTRACT SECURITY CLASSIFICATION	
☒ UNCLASSIFIED/UNLIMITED ☐ SAME AS RPT. ☐ DTIC USERS	Unclassified	
22a. NAME OF RESPONSIBLE INDIVIDUAL Mr. F.W. Schaekel	22b. TELEPHONE (Include Area Code) (703)-664-3576	22c. OFFICE SYMBOL STRBE-VF

DD FORM 1473, 84 MAR — 83 APR edition may be used until exhausted. All other editions are obsolete.

SECURITY CLASSIFICATION OF THIS PAGE
UNCLASSIFIED

EXECUTIVE SUMMARY

The United States Army has a number of flexible fiber reinforced polyurethane fuel storage tanks in service or tightly packaged and stored in warehouses. Some of these tanks have been used and stored while others are new. Degradation of the polyurethane components of the tank wall caused by aging and weathering sometimes leads to unexpected failure. It is necessary to evaluate the condition of these stored tanks before placing them into service. A promising, convenient and effective method for field evaluation of these fuel tanks is based upon determining the surface electrical resistivity of the polyurethane coating on the tanks by a portable resistivity meter.

As part of this work directive, SwRI examined urethane samples using Fourier Transform Infrared Spectrophotometry. The samples, furnished by Belvoir Research and Development Center, resulted in good correlation with infrared spectra with exposure time for the polyester urethanes, but poor correlation for the polyether urethane. Also the two materials containing carbon black were difficult to run and to interpret because of various interferences of the carbon black.

A second project goal was to develop instrumented equipment capable of detecting changes in the surface of polyurethane-coated fuel tanks. Commercially available, portable resistivity meters were found to be ineffective in measuring the surface resistivity of solid, cured polymers. A more dependable, sensitive, and quantitative measuring device was conceived and developed at SwRI. This meter was constructed and found to be capable of measuring the surface resistivity of polymers in various degrees of degradation.

An improved design subsequently evolved which will result in a portable, easy to use, and more accurate meter than the model developed during the course of this work. This "field unit" prototype has been designed and is ready for future consideration for construction.

FOREWORD

The work reported herein was conducted at Southwest Research Institute for the Belvoir Fuels and Lubricants Research Facility (SwRI) at Southwest Research Institute, San Antonio, Texas under Contract No. DAAK70-85-C-0007 and covers the period April 1985 through September 1985. Contracting Officer's Representative was Mr. F.W. Schaekel, Fuels and Lubricants Division/STRBE-VF. The Technical Monitor was Mr. Paul Touchet/STRBE-VU.

TABLE OF CONTENTS

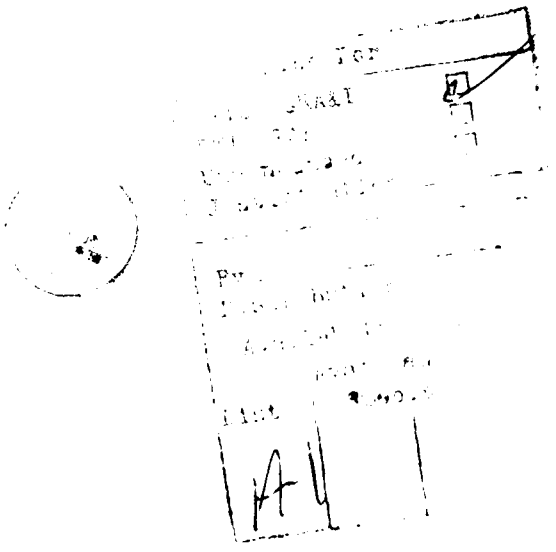

LIST OF ILLUSTRATIONS

LIST OF TABLES

I. INTRODUCTION

Southwest Research Institute (SwRI) was contracted by the U. S. Army Belvoir Research and Development Center to examine urethane samples by Fourier Transform Infrared Spectrophotometry (FTIR). The samples, supplied to SwRI by Belvoir R&D Center, resulted in good success in correlating IR spectra with exposure time for the polyester urethanes, but poor correlation for the polyether urethanes. The two materials containing carbon black were difficult to run and to interpret because of various interferences of the carbon black. A copy of the technical report for this phase is included as Appendix A.

A second phase of this work directive was to develop a nondestructive, field-operated system for evaluating the physical condition of the fiber-reinforced polyurethane fuel tanks used by the Army. The project goal was to develop instrumented equipment capable of detecting changes in the surface of polyurethane-coated fuel tanks indicating that the urethane had undergone degradation and was no longer suitable for use. It was determined that an instrument capable of measuring the surface resistivity of an elastomer would be the most suitable for a quick field check of the condition of the fuel tank. The detection method employed had to be fast, noninvasive, safe to use, and easily operated by unskilled military personnel.

II. BACKGROUND

The U. S. Army is currently using large fiber-reinforced elastomeric bladders or tanks for the storage of fuel or other liquids. These tanks may be folded and stored in crates for years before being used. They may also be stored in their crates for years after being used for fuel storage. Some residual fuel usually remained in the tank after it had been emptied and stored. These tanks are stored in warehouses under a variety of climatic conditions, including hot, humid ones. This combination of heat and humidity is deleterious to the urethane used in the construction of the tanks. For handling ease and for saving warehouse space, these tanks are tightly folded

and packed into wooden crates. Stress concentrations result along the folds and creases of the tanks during storage due to the tight packaging. The combination of extended storage in a hostile climate, extended contact with hydrocarbon-based fuels, and tight packaging can lead to premature failure of the elastomeric tanks.

Unless a crack or failure point were plainly evident, an unreliable tank could be filled with highly flammable fuel. If a major leak occurred in the tank wall, the results could be catastrophic and deadly. Also if the leak were to occur in a fuel tank being used in a combat situation, the loss of fuel could deprive forward combat units of sorely needed fuel for armor support and impair their mobility. Even if filled with water, a very large tank could present a hazardous situation if it were to suddenly rupture.

To prevent an unsafe tank from being put into service, they should be tested before use. One way to check their integrity would be to fill the tanks with water or air prior to use. However, a check of this nature would be time-consuming, expensive, and impractical for very large tanks. Another method would be to inspect the tank wall in various places to determine the suitability of the tank for use. The elastomer structure of the tank wall could be analyzed for scissions in the polymer chain or a breakdown of the cross-linked structure. The polymer could be examined for visible changes in light absorption, reflection, or efflorescence at different light frequencies. The tank structure could also be tested for changes in mechanical behavior such as tensile strength changes. However, the above mentioned analytical techniques to evaluate the condition of the fuel tank all require laboratory facilities. The tank wall must then be patched at those sample points, introducing potential weak spots in the tank. Normally, a large number of samples would be required to accurately determine the condition of the tank and would render the aforementioned invasive and destructive analytical techniques impractical.

An optimum technique for determining the condition of the urethane used in the fuel tanks would be fast, nondestructive, and reliably performed in the field by Army personnel. Based upon these criteria, it was decided to employ an

instrumented method using a resistivity meter to evaluate the condition of the urethane used in the fiber-reinforced fuel tanks. This resistivity meter had to be capable of measuring the specific electrical resistivity or conductance of the polymer surface. A dramatic decrease in the surface resistivity of the urethane used to make the fuel tank would indicate the polymer had degraded and the fuel tank wall could fail.

III. PROCEDURE

The goal of this study was to develop a noninvasive and nondestructive method to determine the condition of the polyurethane component of fiber-reinforced polyurethane fuel tanks. The method developed during this program was based upon measuring the surface resistivity of polyurethane. Samples of humid aged polyurethane samples received from Ft. Belvoir were tested to correlate resistivity data with the duration of humid aging of the samples. The polyurethane specimens received from Ft. Belvoir are listed in Table 1. A change in the polymer due to aging could cause a change in surface resistivity of that polymer. Samples of polyurethane-coated fabric were also received from Ft. Belvoir. These specimens were not subjected to accelerated aging. The surface resistivity was measured to test the effectiveness of the SwRI method on the textured, grainy surface found on the fuel tanks. The results of the resistivity measurements taken at SwRI can be compared to physical strength data gathered at Ft. Belvoir which is shown in Figure 1. This comparison of electrical resistivity to physical strength for each of the humid aged specimens should indicate if electrical resistivity could predict the physical strength of the polymer.

There were two major tasks or steps involved in developing an instrumented method for checking the surface resistivity of the polyurethane. One task required the development of a technique for taking resistivity measurements on the surface of the polyurethane. This technique had to be suitable for use in field operations by unskilled personnel. Another task involved the development of an instrument capable of measuring the surface resistivity of

TABLE 1. POLYURETHANE SAMPLES FOR SURFACE RESISTIVITY MEASUREMENTS RECEIVED FROM FT. BELVOIR

Humid Aged*

Sample	Type	Days Humid Aged
A-1	Polyester-based	0 control
A-2		7
A-3		14
A-4		28
B-1	Polyester-based	0 control
B-2		7
B-3		14
B-4		28
B-5		42
B-6		70
C-2	Polyether-based	0 control
C-2		14
C-3		28
C-4		42
C-5		70
PU-1-1	Polyester-based,	0 control
PU-1-2	carbon filled	7
PU-1-3		14
PU-2-1	Polyether-based	0 control
PU-2-2	carbon filled	7
PU-2-3		14
PU-2-4		28
PU-2-5		42
PU-2-6		70

*Humid aging consisted of immersion of coupon into water at 160°F

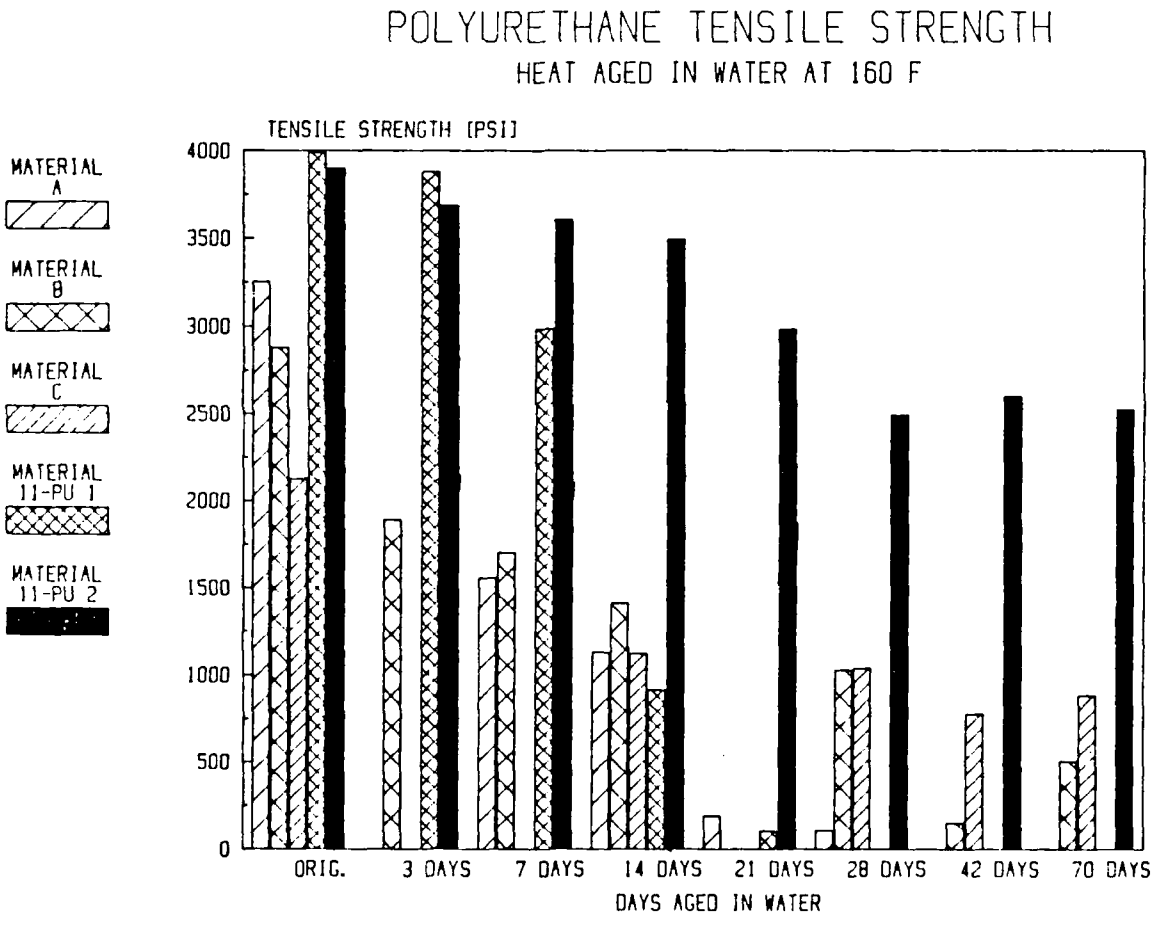

Figure 1. Physical Strength Data Supplied by Fort Belvoir

polymers. Like the technique, this instrument had also to be suited for use in field operations by unskilled personnel. In addition, this meter had to be portable and to deliver accurate and reproducible results. Although it was preferable that the instrument selected for testing be commercially available, no suitable meter was listed in commercial catalogs; therefore, one was designed and built at SwRI. The design specifications and parts list are shown in Appendix B.

A. Surface Preparation

The first step in taking surface resistivity measurements was to clean and prepare the surface of the polyurethane samples. Three cleaning methods were investigated. They involved cleaning with (1) detergent, (2) solvent, and (3) mild abrasive. The detergent was a common household dishwashing detergent, and the solvent was methyl ethyl ketone (MEK). A commercially available mild abrasive pad was also used. After scrubbing with the detergent or the abrasive pad, the samples were rinsed with water to remove all residue and then wiped dry. These three cleaning methods were tested because one cleanser may not be suitable for all types of surface contamination.

There was some concern that cleaning the polyurethane tank surface would remove too much of the damaged polymer surface, thus destroying any possibility of meaningful surface measurements. It was decided, however, that if the deteriorated portion of the polymer surface could be sloughed off merely by washing, then very little subsurface degradation had occurred and the tank was still suitable for use. On the other hand, if the damage to the polyurethane was extensive and extended deeply into the polymer structure, then washing of the surface would not remove all the damage and would not abrogate surface resistivity measurements.

After the polyurethane specimens were cleaned and free of any contaminants that could contribute to ionic activity on the polymer surface, they were ready for surface resistivity measurement. To make these measurements, a probe connected to a conductivity meter was placed upon the polymer surface and a resistivity reading was recorded.

Two methods were evaluated for taking resistivity measurements. One method required the application of deionized water to the surface of the polymer before the meter probe was placed in contact with the polymer. The other method for measurement required a dry polymer surface painted with silver-filled paint.

To ensure consistent resistivity measurements when using the method requiring deionized water, a constant volume of water on the polymer surface was needed. This water had to remain in place on the polymer surface while measurements were taken. Two ways to contain a known volume of water on the surface of a nonabsorbent polymer were tried. One way to try to hold water on a polymeric surface was to gel the water; another way was to build a containment dam.

The compounds to gel deionized water were tested for their effect on he conductivity of the water. To be of use in taking surface resistivity measurements, the gelled deionized water must be nonconductive. The gelling agents which were tested were:

Colloidal silica
Guar gum
Methyl cellulose (nonionic)
Ethyl cellulose (nonionic)
Carbopol 834
Polyvinyl alcohol
Bentonite
Carbowax 6000

The other way used to try to contain a known and constant volume of deionized water on the surface of a polyurethane specimen was to build a dam to hold that water. The materials used for making this dam could not have any water-soluble ions that would affect the ionic activity of the water. The following materials to build a dam were investigated:

Plumbing wax
Modelling clay
Paraffin
Paraplast (polymer-treated paraffin)
Silicone Rubber RTV

The ionic activity of the gelled water and the water contained by the dam were tested by a conductivity meter and a volt-ohm meter. The meter probe tip was placed in the water and a conductivity measurement was obtained.

An alternate method using silver-filled paint for preparing the surface of the polymer for resistivity measurements was developed. With this technique, the cleaned specimens were painted with a conductive silver paint that is also used for printed circuits. The silver paint was used as electrodes on the polyurethane surface. Prior to painting, a circular decal of the type used in printed circuits was placed upon the specimens. The area inside the circle and outside the circle were then painted with the silver paint. After the paint had dried, the decal was removed, leaving an unpainted annulus between the specimen as shown in Figures 2 and 3. Specimen preparation is covered in greater detail in the Operating Procedure section of Appendix B. For surface resistivity measurements, meter probes were placed upon the painted portion of the specimen with one probe tip placed in each painted area surrounding the unpainted annulus, as shown in Figure 4.

B. Meter Evaluation

For the proposed test method that involved the use of water, any instrument used had to measure polymer surface resistivity as well as the electrical resistivity of water. Two types of instruments for measuring the conductivity of water and the surface resistivity of polyurethane were originally planned for evaluation. These meters were commercially available and were used primarily to check the conductivity of deionized water and the gelled deionized water. One of these instruments was the Hewlett-Packard 3465A Digital Multimeter, a volt-ohm meter capable of measuring up to 20 megaohms of resistivity and 10 microvolts of current. The other meter was a conductivity

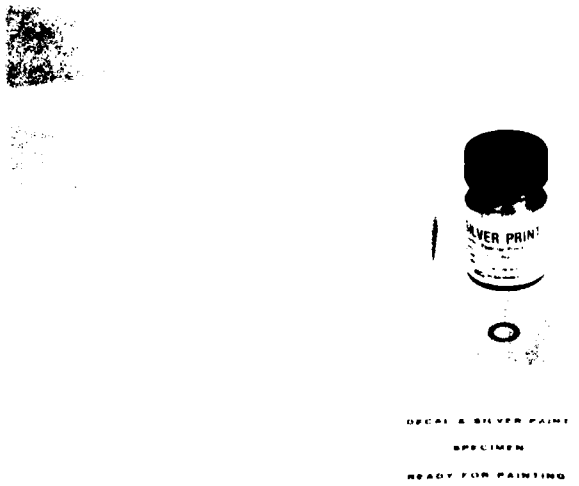

Figure 2. Unpainted Specimen Showing Decal Ring, Silver Paint, and Applicator

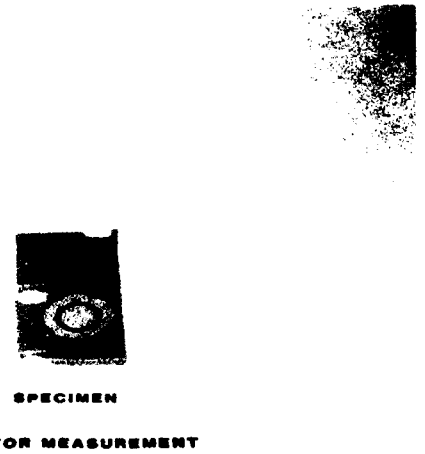

Figure 3. Polyurethane Specimen Showing Inner and Outer Silver Paint Electrodes and Unpainted Annulus

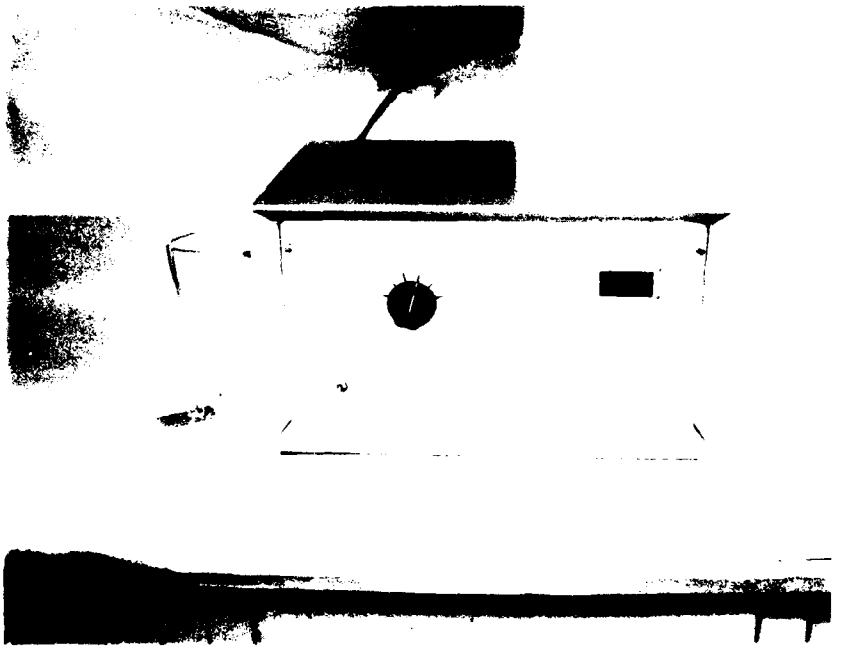

Figure 4. Capacitance-Charging Meter with Specimen Positioned for Measurement

meter manufactured by Lawson Electronics. When each of these meters was used, it was coupled to a probe having two metal tips spaced 0.5 inch apart. This probe was placed in a polyethylene beaker containing 100 grams of deionized or gelled deionized water. The conductivity measurements were performed at room temperature. Additionally, the meters were used in an attempt to take surface resistivity measurements on dry urethane samples that had been cleaned by one of the aforementioned cleaning methods. For this application, the probe tips were placed upon the surface of the polymer and gently pressed down to maintain adequate surface contact.

After work using the Hewlett-Packard and Lawson meters was completed, a catalog search of available conductivity meters was performed. It was determined that commercially available meters were designed to measure the conductivity of liquids but not solid polymers. No portable meter for measuring the surface resistivity of polymers was found in any literature. Upon consultation with a staff member in the Instrumentation and Space Research Division, it was decided that SwRI could build a resistivity meter using inexpensive, commercially available parts. Two types of meters were designed. One meter was based upon a capacitance-charging principle and the other upon a voltage-divider principle. The voltage-divider instrument is supposed to be more accurate and better suited for field use than the capacitance-charging meter. Both instruments are described in greater detail in Appendix B. The capacitance-charging meter was chosen for this study because all the parts were available while some of the parts used in the voltage-divider instrument would have had to be back ordered and could not have been received in time to complete the project on schedule.

IV. RESULTS AND DISCUSSION

The results of the work performed in this program are presented in two parts based upon the test procedure cited in Section III of this report. Some of the testing was qualitative in nature while some was quantitative.

A. Surface Preparation and Evaluation

The polyurethane laboratory specimens as received from Ft. Belvoir appeared clean and were probably not indicative of the condition of the surface of any fuel tanks that have seen extended use and storage. However, they were washed with the three types of cleaning methods to determine if any of these cleaning methods were deleterious to the polymer. The use of solvents that would attack polyurethane or strong abrasives that would scrub away much of the polymer coating on a fuel tank would not have been advisable. The three methods used in this study for surface cleaning were chosen because they did not damage the polyurethane, yet were effective in removing grease, waxes, salts, soil, or general grime. The type of cleanser chosen in the field would depend upon the type of contamination present. In some cases, such as a tank surface contaminated with a thick coating of greasy dirt having a high salt content, all three methods could be used to clean an area for testing. Cleaning with the abrasive pad or liquid soap should always be followed with at least three deionized water rinses to remove any abraded material or soap. After cleaning an area with any of the three cleaners, the area should be wiped with a clean, dry cloth.

The use of deionized water or gelled deionized water for taking resistivity measurements presented a number of problems. All of the gelling agents listed in Section III.A proved to be too ionic in nature when added to deionized water. The gelled water became far too conductive to be used as a medium for determining the surface resistivity, or conductivity, of a polymeric substance. This effort was abandoned.

The materials listed in Section III.A for forming a dam to hold deionized water on the polymer surface were equally unsatisfactory. Only the modelling clay formed a watertight barrier against the surface of the polymer, but it contained some water-soluble compounds. The other four materials tried did not form a watertight seal when applied to the surface of a polymer and also contaminated the test water. Even if satisfactory performances were obtained from some of these materials, their use in the field would be difficult and inadvisable. This effort was also abandoned.

Painting the specimens with silver paint to form electrodes on the polymer surface proved to yield meaningful resistivity readings. Care had to be taken when painting the specimens to ensure that the unpainted annulus was of uniform width. This uniformity is essential because the surface resistivity is measured across the unpainted gap between the two painted electrodes; therefore, differences in annulus width would result in different resistivity measurements. The application of silver paint to the textured and grainy fabric-coated specimens was difficult because the paint followed the grain, creating an irregularly shaped annulus between the two silver paint electrodes. See Figure 5. This irregularity would result in inconsistent and useless resistivity measurements. Also, care had to be exercised not to apply too much paint thus allowing the paint to follow the grain of the fabric at the periphery of the unpainted annulus.

B. Meter Evaluation

Although the Hewlett Packard 3465A Digital Multimeter was capable of measuring a large amount of resistance and a small amount of current, it was not capable of surface resistivity measurements or measurement of the resistivity of deionized water. The current flowing through the instrument during use polarized the water or polymer surface in the area surrounding the probe tips. The degree of polarization was constantly varying; therefore no meaningful resistivity measurements were taken. The meter was determined to be unusable for this application, and no further work was done using it.

Although the Lawson electronic meter was capable of detecting changes in the conductivity of water, it was designed to give qualitative measurements only. It was useful in determining that all of the additives for gelling deionized water increased the conductivity of that water. The Lawson conductivity meter was not designed to measure surface resistivity of polymers. Work involving this meter was also cancelled.

The capacitance-charging based meter developed at SwRI was consistently able to measure the relative resistivity of all the humid aged specimens provided by Ft. Belvoir. From these relative readings, the specimens were ranked

Figure 5. Textured Urethane Coated Fabric

according to the duration of exposure to 160°F water for each of the five specimen types. Multiple resistivity readings were taken on three different days to check the reproducibility of the meter readings. In all cases, the resistivity readings were similar to those measurements taken the preceding day. The instrument was consistently able to define the difference in resistivity of the urethane samples and enabled the operator to correctly rank the specimens according to the amount of humid aging exposure each sample of one type received, as shown in Table 2. These data are also represented graphically in Figures 6 through 10. For the urethane specimens not containing carbon black, only a couple of inconsistencies occurred in the data as can be seen in Figures 9 and 10. These anomalies in the data were for those specimens aged only 14 days. For those specimens humid aged for a longer period of time, the resistivity readings were consistent with respect to those obtained on the other specimens of the urethane type. As expected, the urethane specimens not containing carbon black exhibited a decreasing resistivity as the specimen exposure time increased. This decrease in resistivity, or increase in conductivity indicates that a chemical change such as chain scission or cross-link bond breaking has occurred. A comparison of the resistivity data with the tensile strength data provided by Ft. Belvoir showed a definite correlation between exposure time and tensile strength/ resistivity measurement. See Figure 1 and Figures 6 through 10.

For those specimens containing carbon black, the surface resistivity data were consistent with the duration of exposure of the specimen. Again the specimens were correctly ranked according to length of humid aging exposure. However, the resistivity readings obtained from the samples containing carbon black did not follow the same pattern of decreasing resistivity as did those readings obtained from the urethane specimens not containing carbon black. In fact, the resistivity readings for those specimens containing carbon black increased consistently with increasing exposure to humid aging.

Although the polymer surface resistivity data obtained by using the SwRI-designed meter were relative and not absolute, they did indicate the usefulness of that meter in predicting the degree of humid aging exposure and physical and resultant physical degradation for each of the urethane specimens.

TABLE 2. RESISTIVITY MEASUREMENTS

Sample ID	Type	Days Humid Aged	Resistivity Reading Megaohms/cm^2 Range	Median	Meter Range
A-1	Polyester-based	0 control	4913- 5858	5508	10^{10}
A-2		7	3171- 3803	3592	10^{10}
A-3		14	3805- 4783	4238	10^{10}
A-4		28	640- 762	702	10^{10}
B-1	Polyester-based	0 control	4063- 4990	4433	10^{11}
B-2		7	2012- 2562	2352	10^{11}
B-3		14	4143- 5662	4683	10^{11}
B-4		28	1240- 1933	1413	10^{11}
B-5		42	163- 223	193	10^{11}
B-6		70	32- 40	33	10^{11}
C-1	Polyether-based	0 control	23820-77080	34500	10^{11}
C-2		14	7242- 9662	8243	10^{11}
C-3		28	1583- 2302	2039	10^{11}
C-4		42	1435- 2392	1932	10^{11}
C-5		70	1297- 2193	1788	10^{11}
PU-1-1	Polyester-based,	0 control	32- 102	33	10^{9}
PU-1-2	carbon filled	7	333- 553	442	10^{9}
PU-1-3		14	843- 1682	1063	10^{9}
PU-2-1	Polyether-based,	0 control	592- 673	610	10^{9}
PU-2-2	carbon filled	7	583- 712	700	10^{9}
PU-2-3		14	797- 1202	692	10^{9}
PU-2-4		28	958- 1063	1061	10^{9}
PU-2-5		42	1173- 2062	1672	10^{9}
PU-2-6		70	1940- 2150	2080	10^{9}

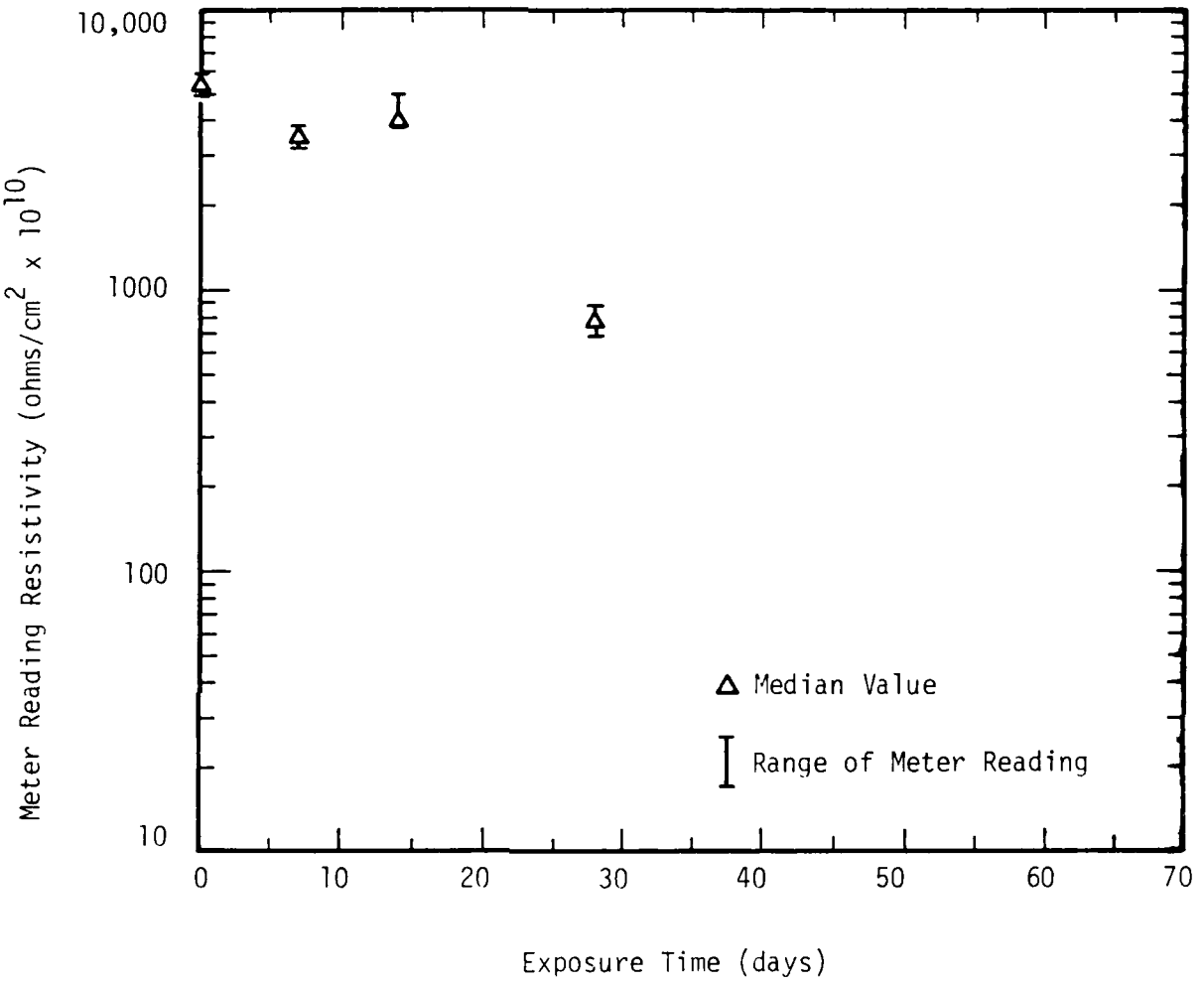

Figure 6. Specimen A

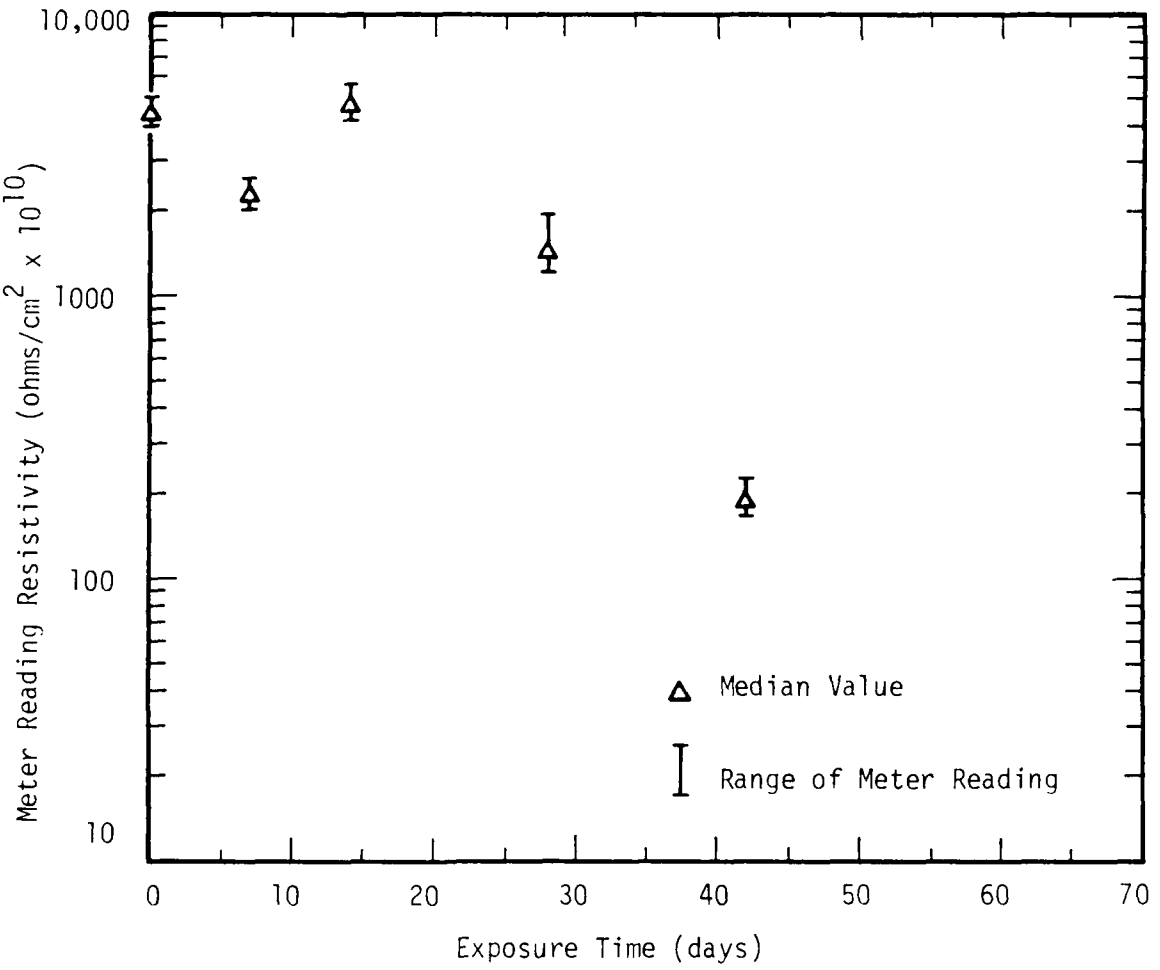

Figure 7. Specimen B

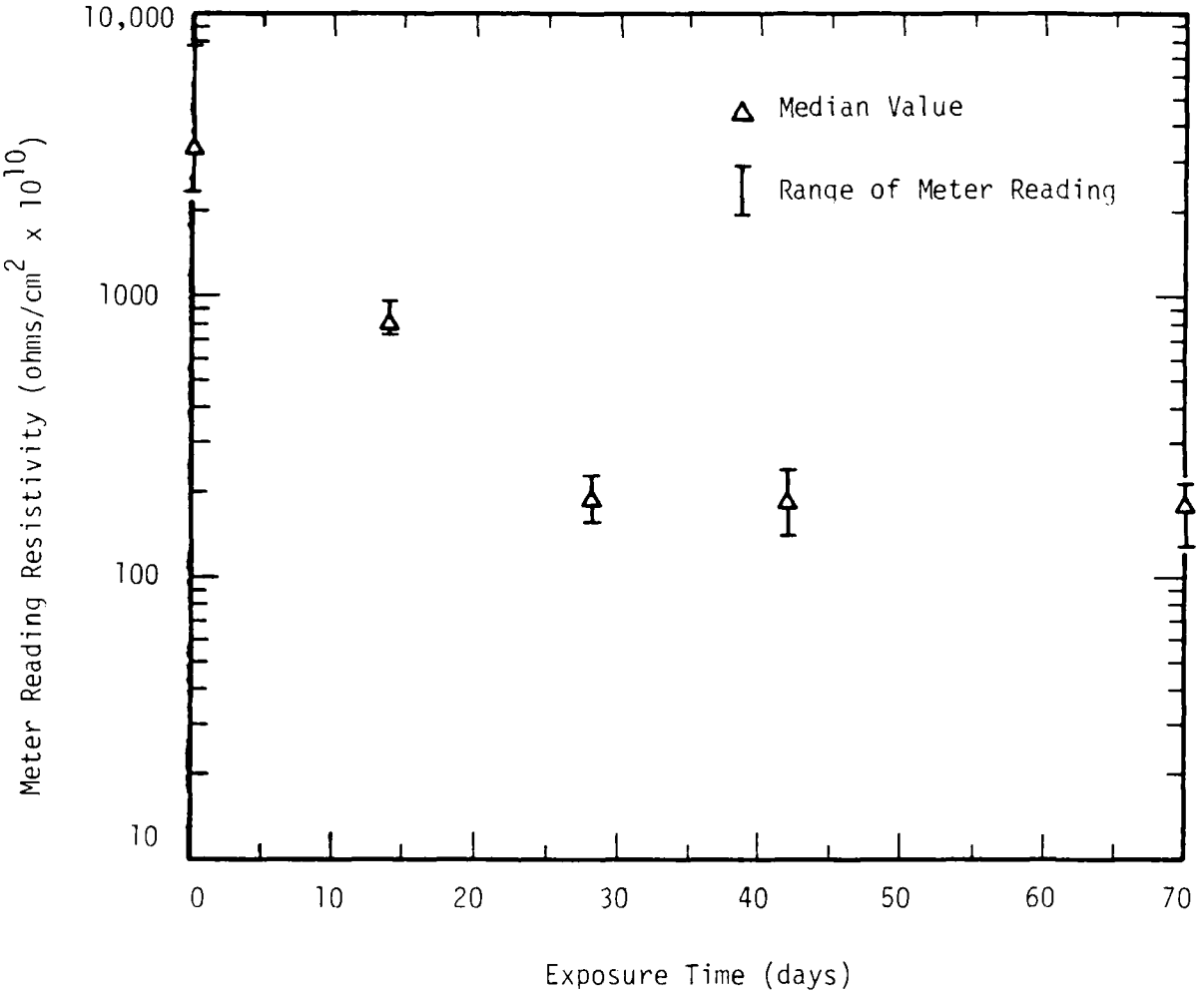

Figure 8. Specimen C

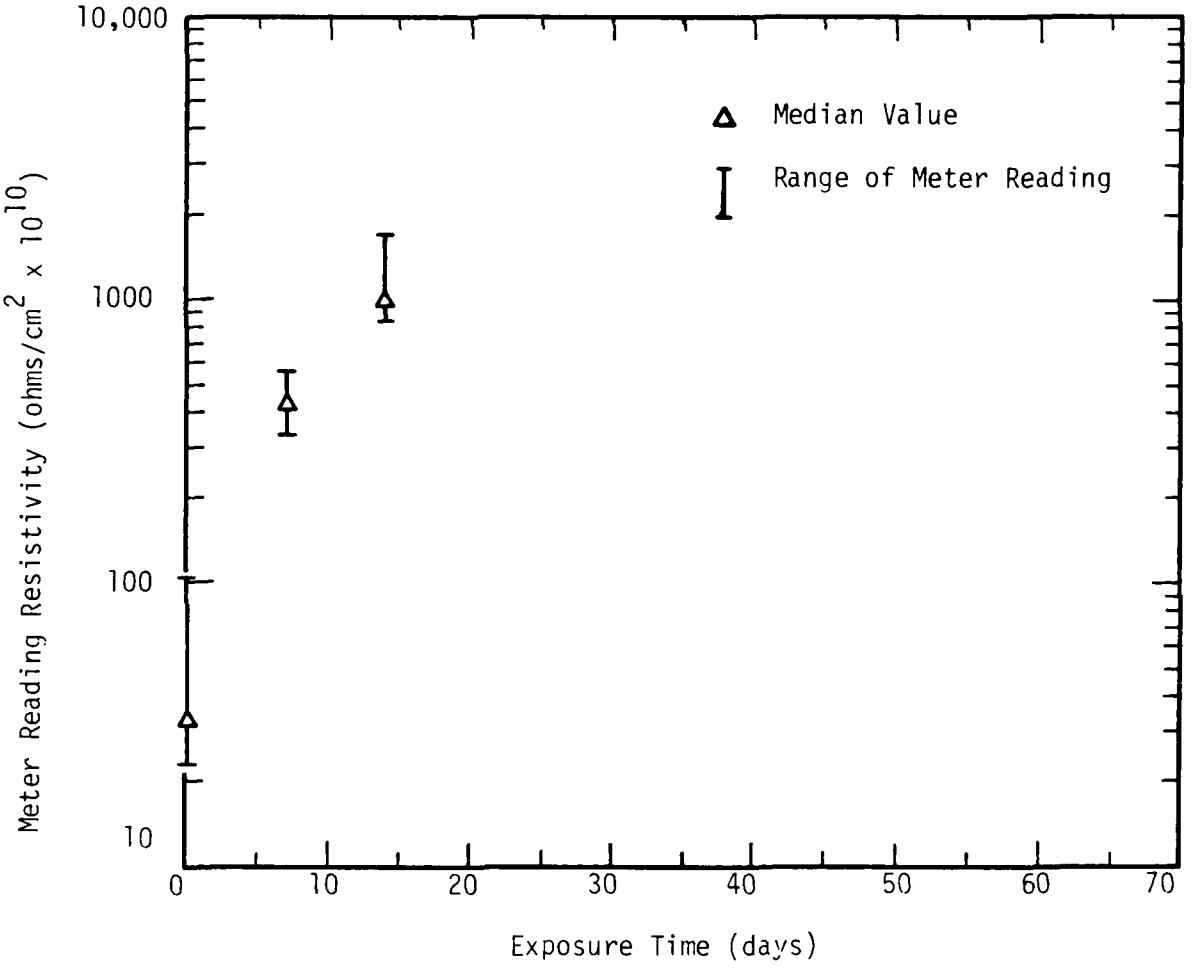

Figure 9. Specimen PU-1

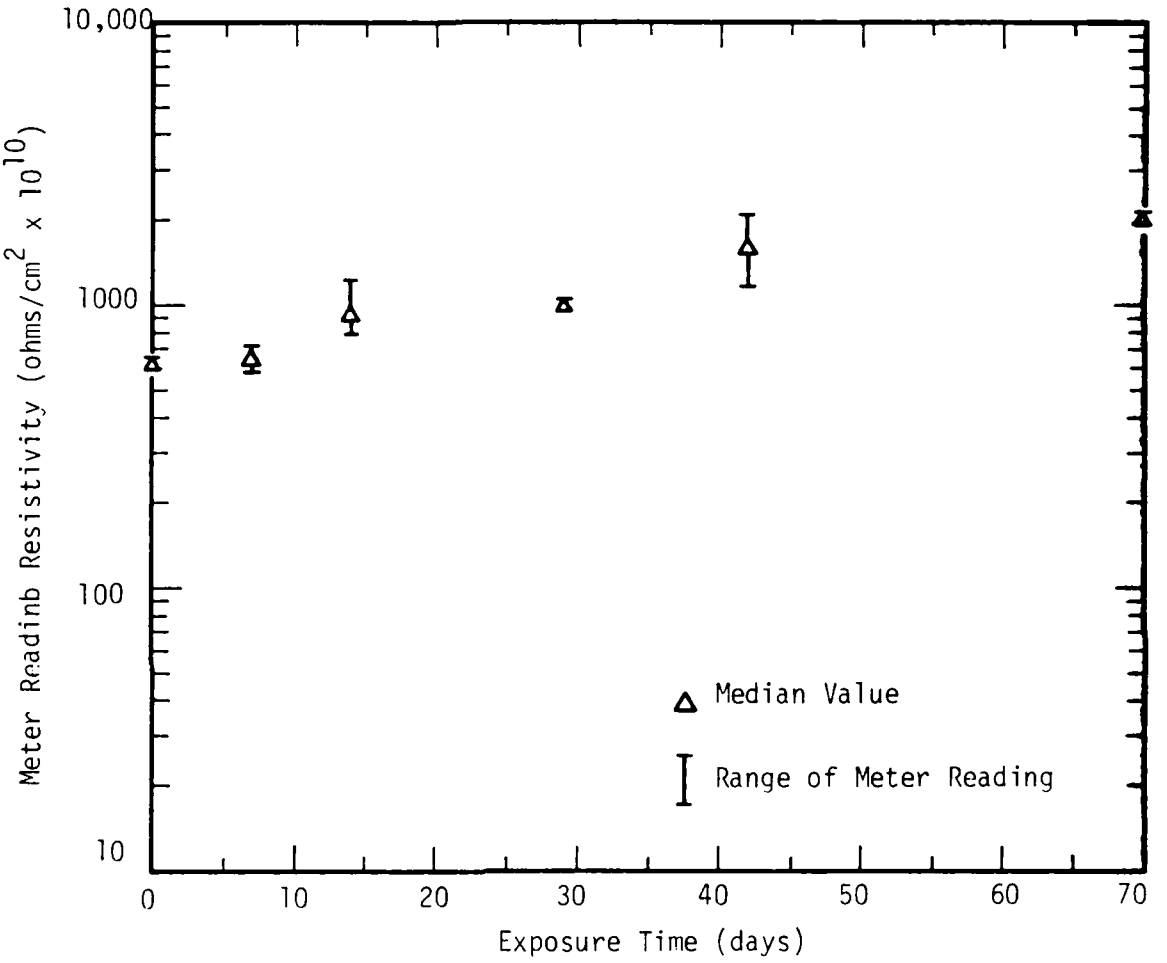

Figure 10. Specimen PU-2

V. CONCLUSIONS

As seen from the data, the SwRI-designed capacitance-charging resistivity meter was a useful tool in predicting the relative amount of humid aging exposure and physical degradation for each specimen within a specific type of urethane. Although this meter was not very suitable for field use, good results were obtained in the laboratory. The data derived from using this meter indicated the feasibility of using a surface resistivity meter to determine the condition of the urethane polymer coating on a coated fabric fuel tank.

The use of water or water-containing gelling agents was difficult, at best, in a laboratory setting. It would be even more difficult to use in the field, provided suitable gelling or containment materials could be found. Further study of the use of water as a transmission medium for resistivity measurements is not recommended.

A second prototype meter is planned that will be portable, accurate, easy to use, and suitable for field use. This meter, based upon the voltage-divider principle instead of capacitance charging, is explained more fully in Appendix B. The next phase of this work will be directed toward development of this meter.

It is expected that the resistivity meter employing the voltage-divider principle will not require the use of silver paint to form electrodes on the surface of the polymer. When using the meter based upon the capacitance charging principle, it was necessary to use electrodes made of silver paint on the polymer surface to greatly increase the amount of surface contact area of the polymer being measured. Unlike the small diameter probe used with the capacitance-charging meter, the probe used with the voltage-divider instrument will have a very large surface area tip, ensuring adequate surface contact with any polymer. This probe tip will simulate the configuration of the silver paint electrodes used with the capacitance-charging meter.

APPENDIX A

FTIR STUDIES OF URETHANE SPECIMENS

FTIR STUDIES OF URETHANE SPECIMENS

I. EXPERIMENTAL

The five sets of specimens were dried in a desiccator several days prior to this study. The infrared spectra of the sample specimens were obtained using a Harrick 4X TBC-VA, set for attenuated total reflectance spectroscopy, on a Digilab Model FTS-15E/D Fourier Transform InfraRed spectrophotometer and the digitized spectra stored for future study. Hard copies of the infrared spectra are presented in Figures 1-24.

Examination of the spectra revealed many abnormalities present in the carbon-hydrogen stretch region (3100 to 2800 cm^{-1}) due to possible contamination by hydrocarbon-like materials and possibly silicone oil release agent. Examination of the spectra revealed slight increases in the absorbence at ca 3300 cm^{-1} (N-H stretch of the carbamate linkage) and the indication of new absorption in the nitrogen-hydrogen and oxygen-hydrogen stretch region between 3600 and 3100. Since these specimens had been exposed to hot water for extended periods the normal degradation of the urethane is expected to be the hydrolysis of the carbamate linkage of the molecule, as illustrated in the equation below, to form amine and alcohol end groups.

$$-[NH\text{-}R\text{-}NH\text{-}\overset{O}{\overset{\|}{C}}\text{-}O\text{-}R'\text{-}O\text{-}\overset{O}{\overset{\|}{C}}]_n + H_2O \rightarrow -[NH\text{-}R\text{-}NH_2 + HO\text{-}R'\text{-}O\text{-}\overset{O}{\overset{\|}{C}}]_n + CO_2$$

The amide II absorption band at ca 1565 cm^{-1} (N-H deformation and C-N stretch of the carbamate linkage) should be decreased by this hydrolysis as well as the N-C-O stretch band at ca 1219 cm^{-1}. In order to evaluate the data obtained area measurements and peak height ratios were made from the stored digitized spectra and peak area and height ratios were calculated and compared for various peak combinations. The ratios obtained which showed promise are reported in Tables 2-5 and are discussed in the section which follows.

II. DISCUSSION OF RESULTS

A. Series 1 Specimens

Table 1 illustrates that this polyester-based urethane yielded several combinations of peak height ratios which were useful for ranking the samples according to their exposure time. Peak area ratios did not yield useful data for these specimens.

B. Series 2 Specimens

With the exception of sample 2-4, useful peak height ratio data (Table 2) was obtained on this polyester-based urethane. Examination of the spectrum of sample 2-4 (exposed 70 days) reveals that this sample is greatly different from the rest of the samples. It has undergone hydrolysis of the ester as well as the carbamate linkages, hence, yielding peak height ratios which do not correlate with the other specimens. (In actual service this "tank" would probably have long since ruptured and spilled its contents).

C. Series 3 Specimens

This polyether-based urethane did not yield much useful data. Of all the peak height and peak area ratios calculated and compared, only the total area of the O-H and N-H stretch regions ratioed against the C-O-C stretch band area yielded values which would correlate with time of exposure (Table 3). Samples 3-5 and 3-4, (42 and 77 hours exposure) failed to correlate at all. The difficulty in obtaining correlations may be due to the increased resistance of polyether-based urethanes to hydrolysis which causes a reduction in the percentage of the carbamate linkages hydrolyzed.

D. Series 4 Specimens

These samples were from a carbon black filled polyester-based urethane rubber. It is very difficult to obtain reflectance type spectra, useful for quantitative measurements, from carbon black filled polymer due to the appearance of derivative shaped peaks (often with near complete band

inversions sometimes referred to as "restrahlen" bands). In addition the carbon black absorbs so much of the infrared energy that only weak absorbence bands result. In spite of these difficulties, Table 4 does list two peak area ratios based on the N-H and O-H stretch region which correlate correctly with time of exposure.

E. Series 5 Specimens

These specimens were prepared from a carbon black filled polyether-based urethane. The quality of the spectra obtained suffered in ways similar to that of the series 4 specimens. Of various peak area and peak height ratios measured, only one peak area ratio and one peak height ratio gave any significant correlation with exposure time. The data in Table 5 shows good correlation for 4 out of 6 samples. The two samples which do not correlate are 5-3 (70 days exposure) and 5-4 (only 14 days exposure). However, if by chance these two samples were accidentally mislabeled, the data would present excellent correlation if one switched the days of exposure data.

IV. CONCLUSIONS

It has been demonstrated that FTIR does show some promise of being a useful tool to evaluate the degree of hydrolysis of various urethane rubber specimens in the laboratory. However, more studies will be required to fully demonstrate this capability. Under present "state-of-the-art", FTIR is still a "laboratory only" technique. It must be compared against other techniques, presently being studied that may be more adaptable to field use. In any future laboratory studies, there are several considerations which should be applied in preparation of samples for analysis. First, the specimens (preferably cut to the same size) should be cleared of any mold release agents, i.e., silicones, by rinsing with trichlorotrifluoroethane followed by drying prior to exposure to hot water, etc. Second, the specimens should be cleaned again with the same solvent after exposure and then dried in a vacuum desiccator for several days. Finally, the specimens should only be handled with oil-free tweezers prior to analysis by attenuated total reflectance.

The use of a photoacoustic detector accessory for FTIR might give better quality spectra in instances where the urethane rubber is carbon black filled.

TABLE 1. SERIES 1 SPECTRA COMPARISONS

Sample Number	Days Exposed	Absorbence (Peak Height) Ratios (From Computer Calc. Abs.- "zero baseline") 1535[1]/1165[3]	1219[2]/1165	1565/1136[3]	1219/1136	(Computer Calc. Ratios- "Two Point Baseline") 1535/1165	1219/1165	1535/1136	1219/1136
1-1	0	0.744	0.925	0.726	0.903	0.813	0.925	0.797	0.906
1-2	14	0.673	0.898	0.653	0.871	0.715	0.892	0.695	0.867
1-3	7	0.696	0.907	0.673	0.876	0.742	0.901	0.717	0.872
1-4	28	0.613	0.873	0.593	0.844	0.639	0.862	0.619	0.835

(1) The 1535 cm^{-1} absorption is the amide II band which consists of the N-H deformation and the C-N stretch band

(2) The 1219 cm^{-1} absorption is the N-C-O stretch band of the carbamate linkage.

(3) The 1165 cm^{-1} and 1136 cm^{-1} absorptions are C-O stretch bands of the ester linkage.

TABLE 2. SERIES 2 SPECTRA COMPARISONS

Sample Number	Days Exposed	Absorbence (Peak Height) Ratios (From Computer Calc. Abs. "zero baseline") $\frac{1535}{1167}$[1][2]	$\frac{1535}{1136}$[2]	(Computer Calc. Ratios "Two Point Baseline") $\frac{1535}{1167}$	$\frac{1535}{1136}$
2-1	0	0.757	0.748	0.816	0.812
2-2	28	0.712	0.703	0.763	0.760
2-3	7	0.744	0.737	0.805	0.803
2-4[3]	70	0.835	0.946	0.999	1.145
2-5	14	0.721	0.717	0.773	0.774
2-6	42	0.688	0.691	0.731	0.743

(1) The 1535 cm^{-1} absorption is the amide II band which consists of the N-H deformation and the C-N stretch bands.

(2) The 1165 cm^{-1} and 1136 cm^{-1} absorptions are C-O stretchbands of the ester linkage.

(3) Sample 2-4 appears to have undergone hydrolysis of both the carbamate and the ester linkages and the absorbence ratios obtained are useless. (Note, however, that one look at the spectrum indicates that the material has undergone a great change.)

TABLE 3. SERIES 3 SPECTRA COMPARISONS

Sample Number	Days Exposed	Peak Areas[1] 3600-3000 cm^{-1}[2]	Peak Areas[1] 1162-899[3]	Ratio: Area 3600-3000 / Area 1162-899
3-1	0	1083.4	6063.4	0.179
3-2	28	1332.1	6812.6	0.196
3-3	14	1245.8	6570.9	0.190
3-4	77	1897.9	9396.7	0.202[4]
3-5	42	1542.2	6249.2	0.247[4]

(1) Peak areas in arbitrary units, were determined by integration by the instrument computer.

(2) The 3600 to 3000 cm^{-1} region includes the N-H stretch band, of the carbamate group, at ca 3280 cm^{-1} plus the O-H and N-H stretch bands of the primary alcohols and amines formed by hydrolysis of the carbamate group.

(3) This region covers the C-O-C stretch of the polyether component at ca 1103 cm^{-1}. Note, however, that if this peak was integrated between 1161 and 970 the areas obtained fail to yield any correlation at all with time of exposure.

(4) These two peaks fail to correlate in the proper order.

TABLE 4. SPECTRA COMPARISONS

Sample Number	Days Exposed	Peak Area Ratios 3490-3070[1] / 1558-1475[2]	Peak Area Ratios 3490-3070 / 1425-1327[3]
4-1	0	1.238	2.248
4-2	14	1.053	1.778
4-3	7	1.210	2.190

(1) The 3490 to 3070 cm^{-1} region includes the N-H stretch band, of the carbamate group, at ca 3320 cm^{-1} plus the O-H and N-H stretch bands of the primary alcohols and amines formed by the hydrolysis of the carbamate group.

(2) The 1558 to 1475 cm^{-1} region includes the amide II band (N-H deformation and C-N stretch) at ca 1535 cm^{-1} plus the aromatic C-C stretch ca 1512 cm^{-1}.

(3) The 1425 to 1327 cm^{-1} region includes, among others, absorption bands at ca 1412, 1375, and 1350. This region was selected on the basis that the peak areas appeared to remain constant and offered a "flat" baseline between 1425 and 1327 cm^{-1}.

TABLE 5. SERIES 5 SPECTRA COMPARISONS

Sample Number	Days Exposed	Peak Area Ratio $\frac{3460\text{-}3090}{1568\text{-}1475}$ (1) (2)	Peak Height Ratio $\frac{3270}{3063}$ (3) (4)
5-1	0	0.245	0.111
5-2	28	0.167	0.515
5-3	70	0.616	0.437
5-4	14	1.439 (5)	1.850 (5)
5-5	42	0.779	0.652
5-6	7	0.475	0.292

(1) The 3460 to 3090 cm^{-1} region includes the N-H stretch band, of the carbamate group, plus the O-H and N-H stretch bands of the primary alcohols and amines formed by the hydrolysis of the carbamate group.

(2) The 1568 to 1475 cm^{-1} region includes amide II bands and the aromatic C-C stretch band.

(3) The 3271 cm^{-1} band due to N-H stretch of the carbamate group plus the N-H stretch of primary amines and bonded OH stretch of primary alcohols.

(4) The 3063 cm^{-1} band represents the strongest of the aromatic C-H stretch bands.

(5) These two samples fail to correlate in the proper order. If the samples were switched the data would correlate very well.

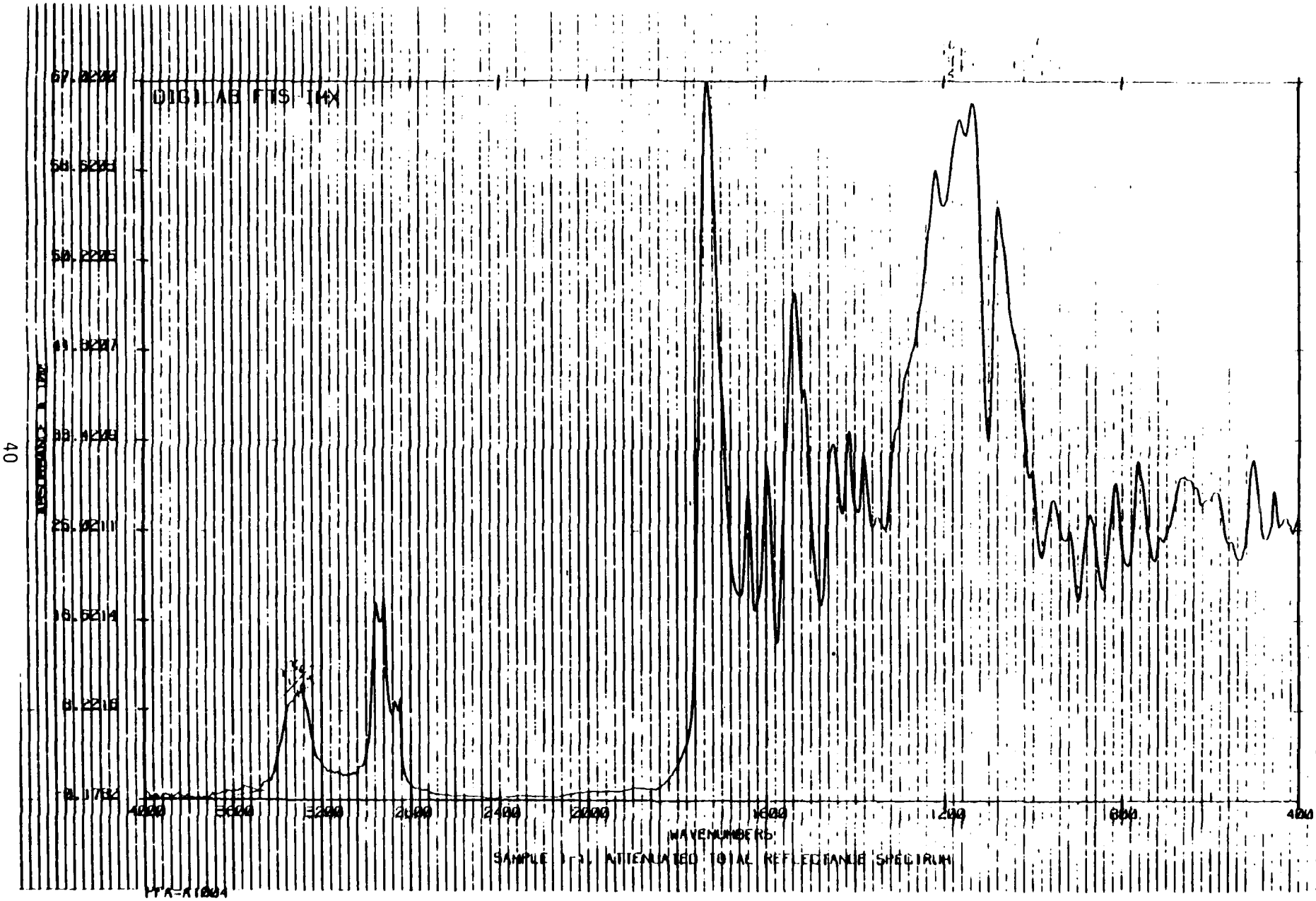
DIGILAB FTIS [4X]
WAVENUMBERS
RES=4 DP
NSCANS=512

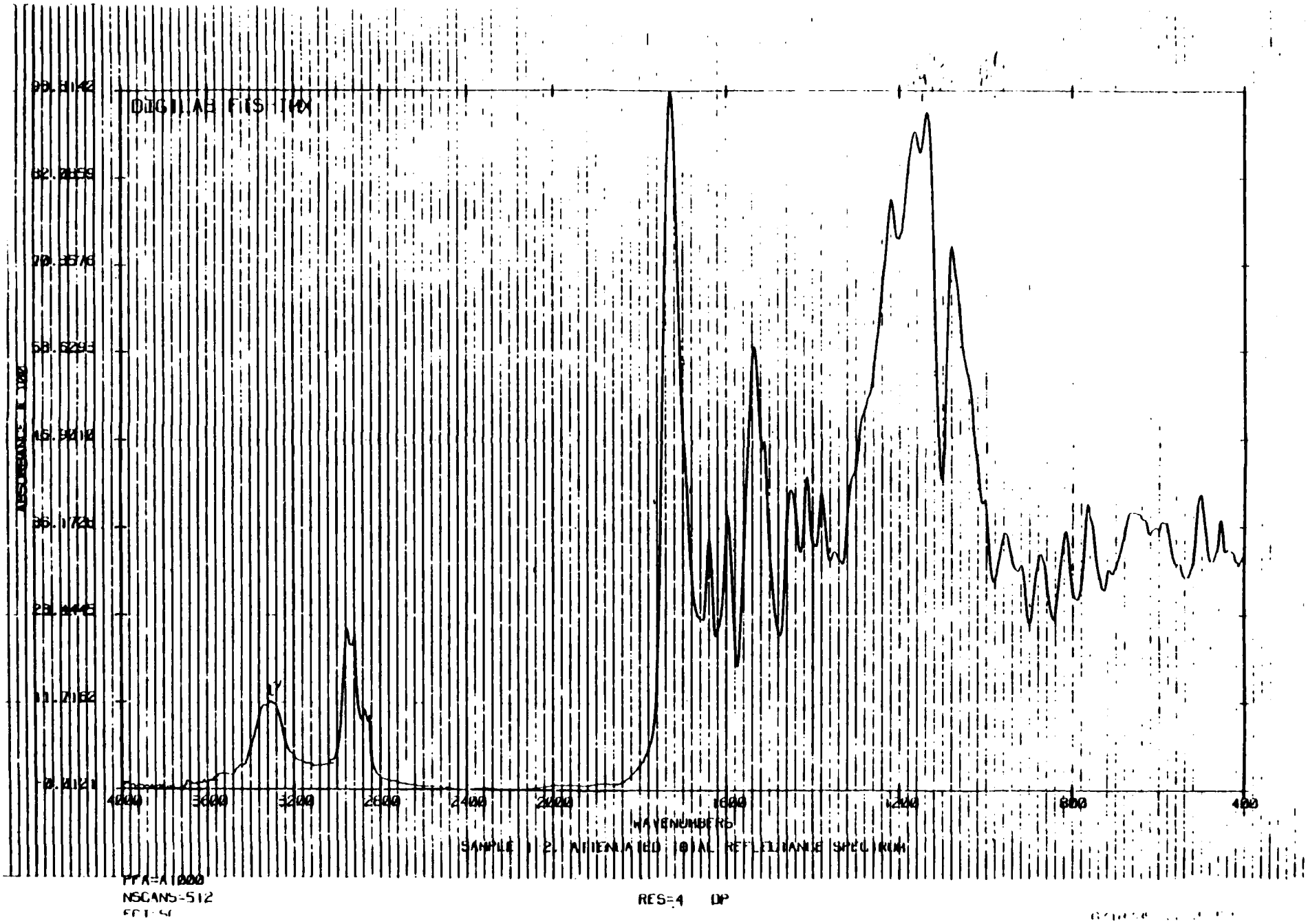
DIGITIAB F(S) (4)
ABSORBANCE
WAVENUMBERS
SAMPLE 1 2. ATTENUATED TOTAL REFLECTANCE SPECTRUM
FFA=A1000
NSCANS=512
RES=4 DP

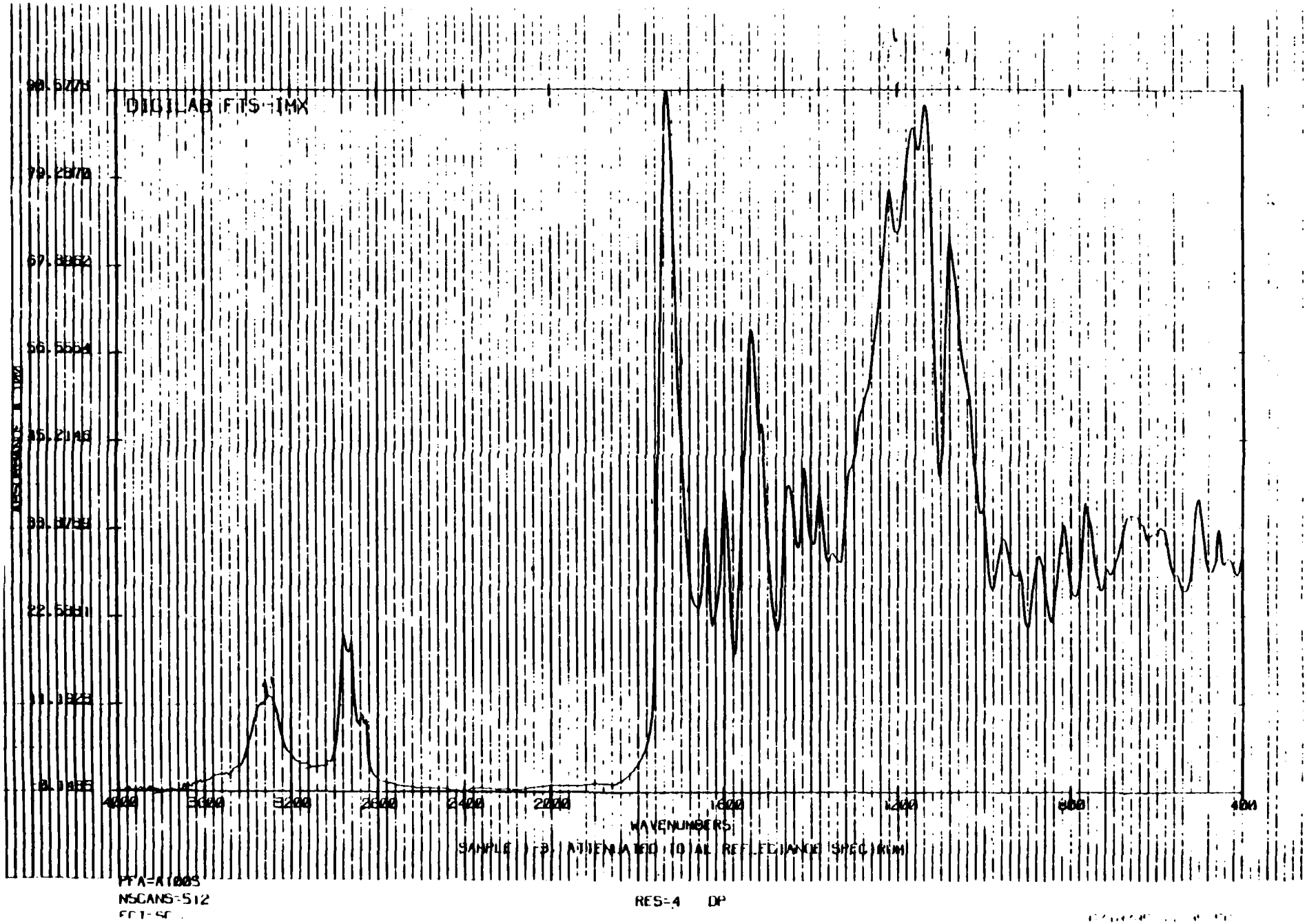
DIGILAB FTS-IMX
WAVENUMBERS
SAMPLE (3) ATTENUATED TOTAL REFLECTANCE SPECTRUM
PTA=A1003
NSCANS=512
RES=4 DP

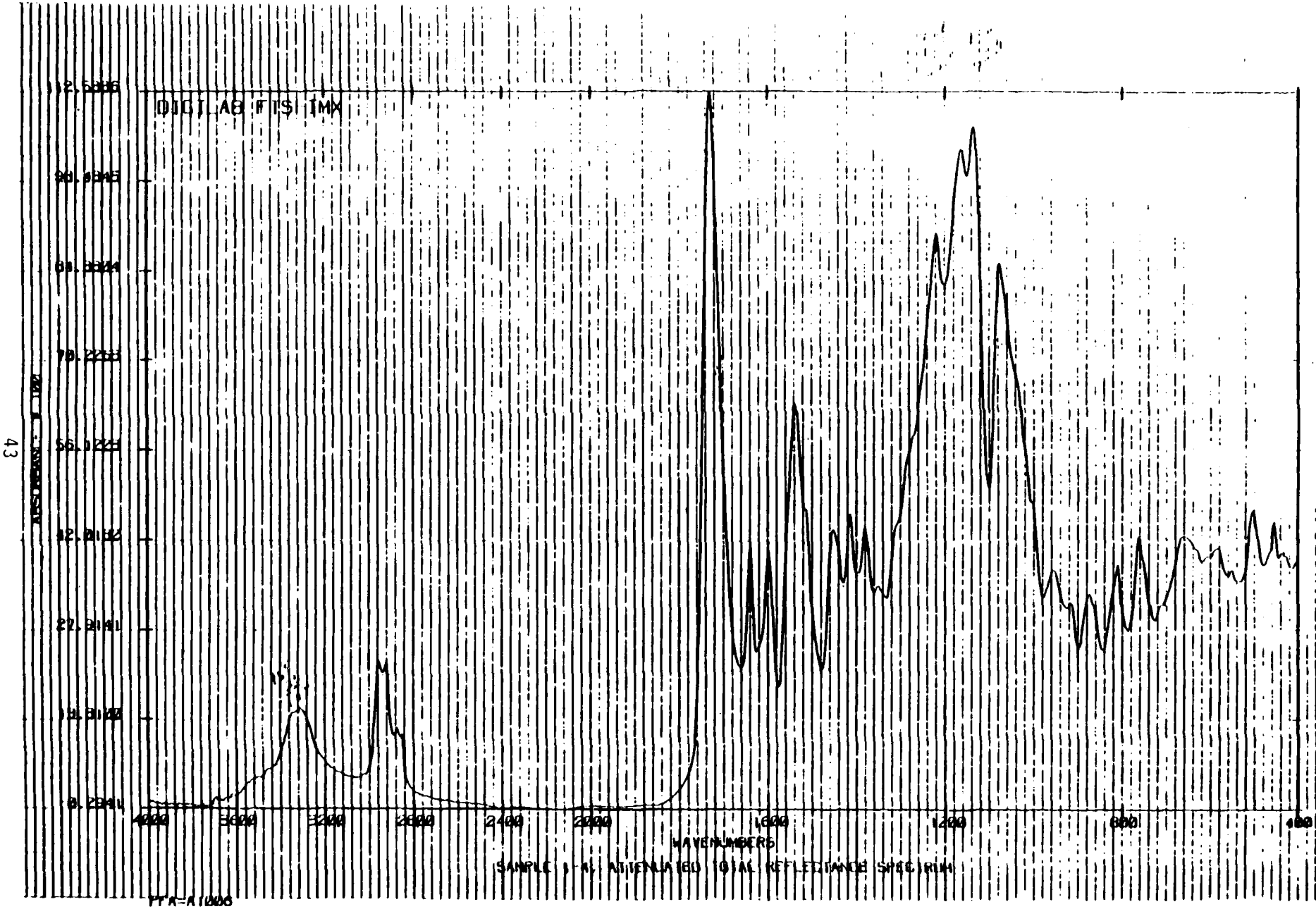
DIGILAB FTS IMX
WAVENUMBERS
SAMPLE 1-A, ATTENUATED TOTAL REFLECTANCE SPECTRUM
RES=4 DP
NSCANS 512

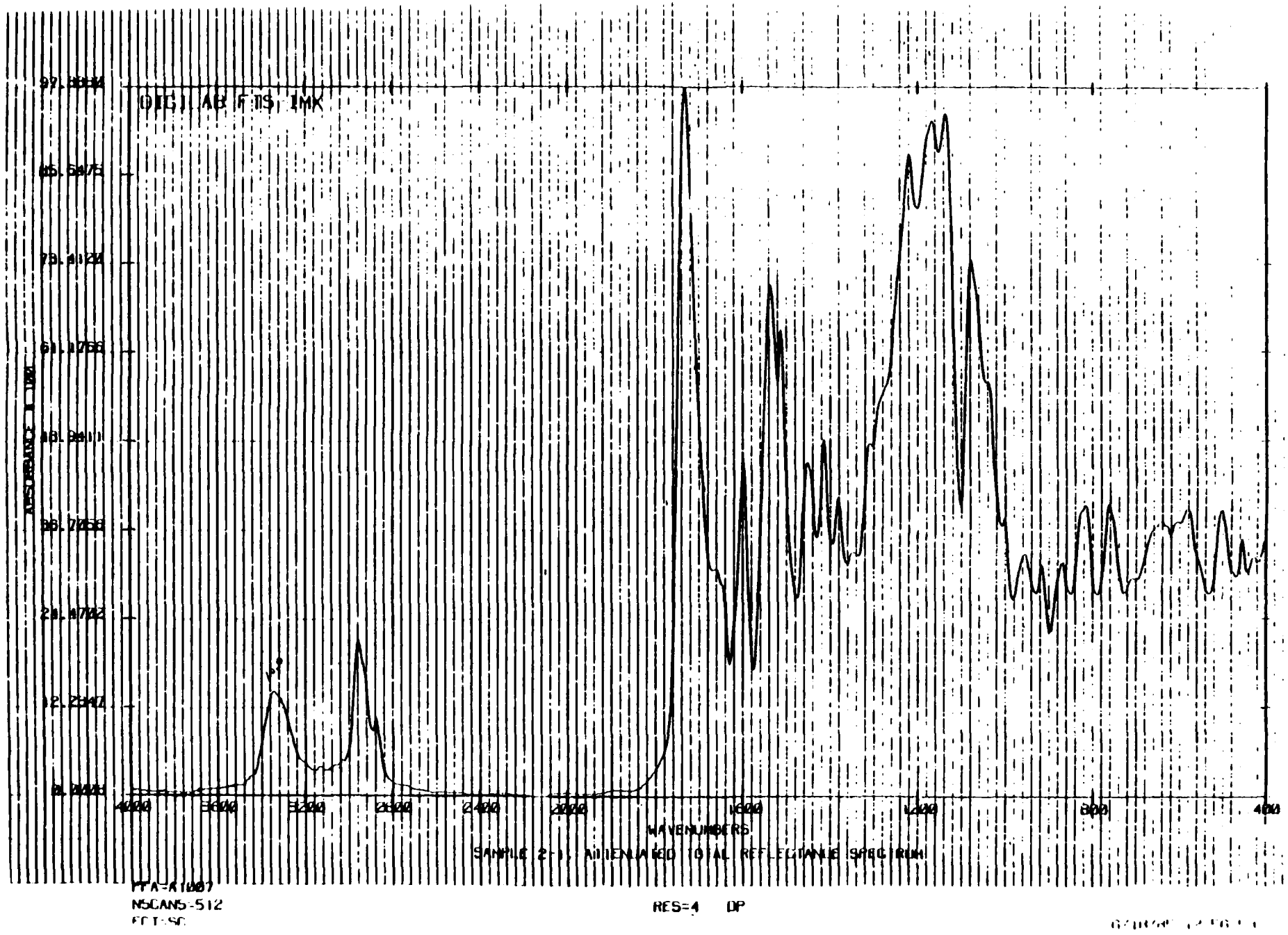
DIGILAB FTS IMK
ABSORBANCE
WAVENUMBERS
SAMPLE 2-1, ALUMINUM COATED TOTAL REFLECTANCE SPECTRUM
FTA-A1007
NSCANS-512
RES=4 DP

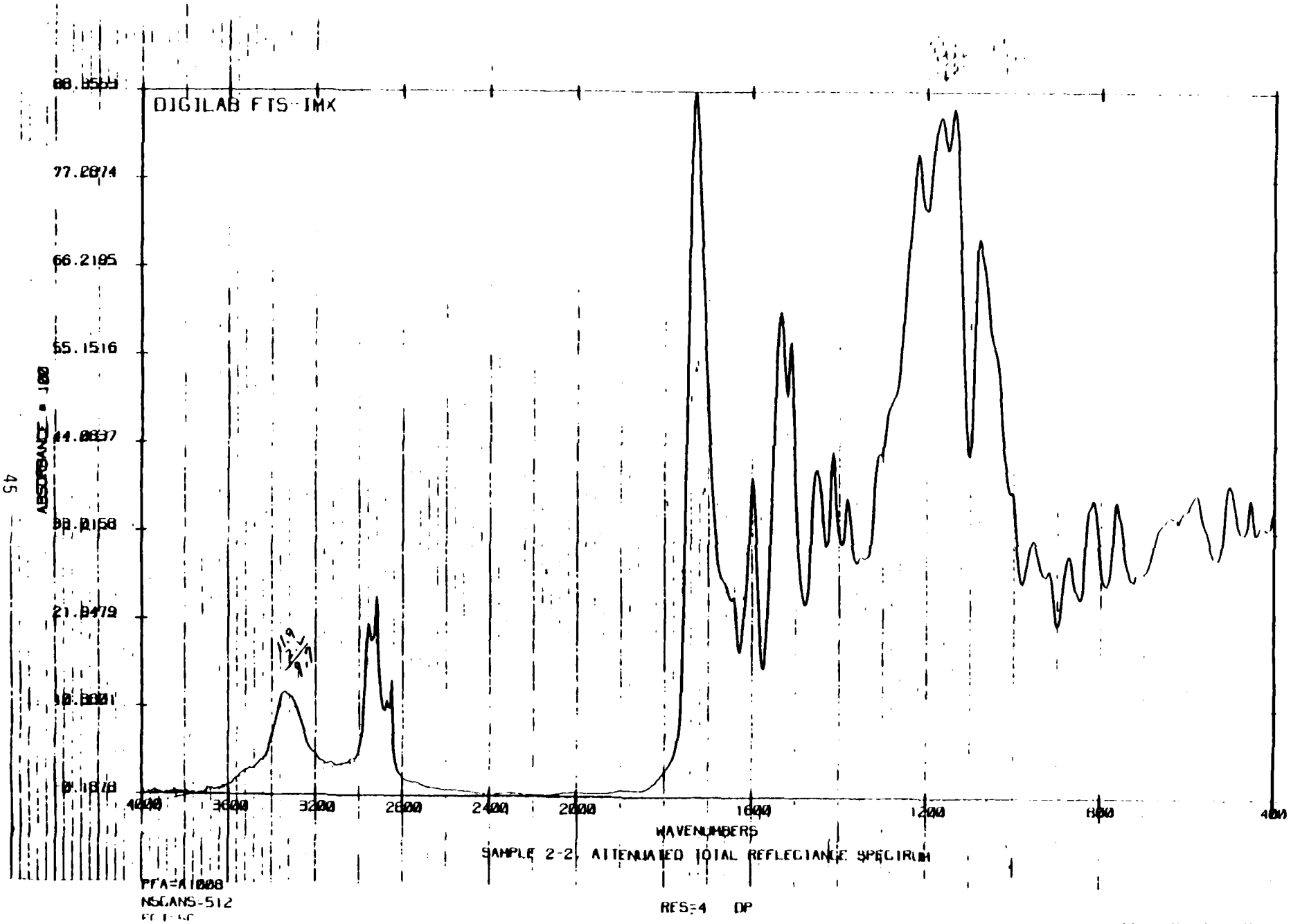
DIGILAB FTS-IMX
77.2874
66.2195
55.1516
ABSORBANCE
1600
1200
800
400
WAVENUMBERS
SAMPLE 2-2, ATTENUATED TOTAL REFLECTANCE SPECTRUM
NSCANS=512
RES=4 DP

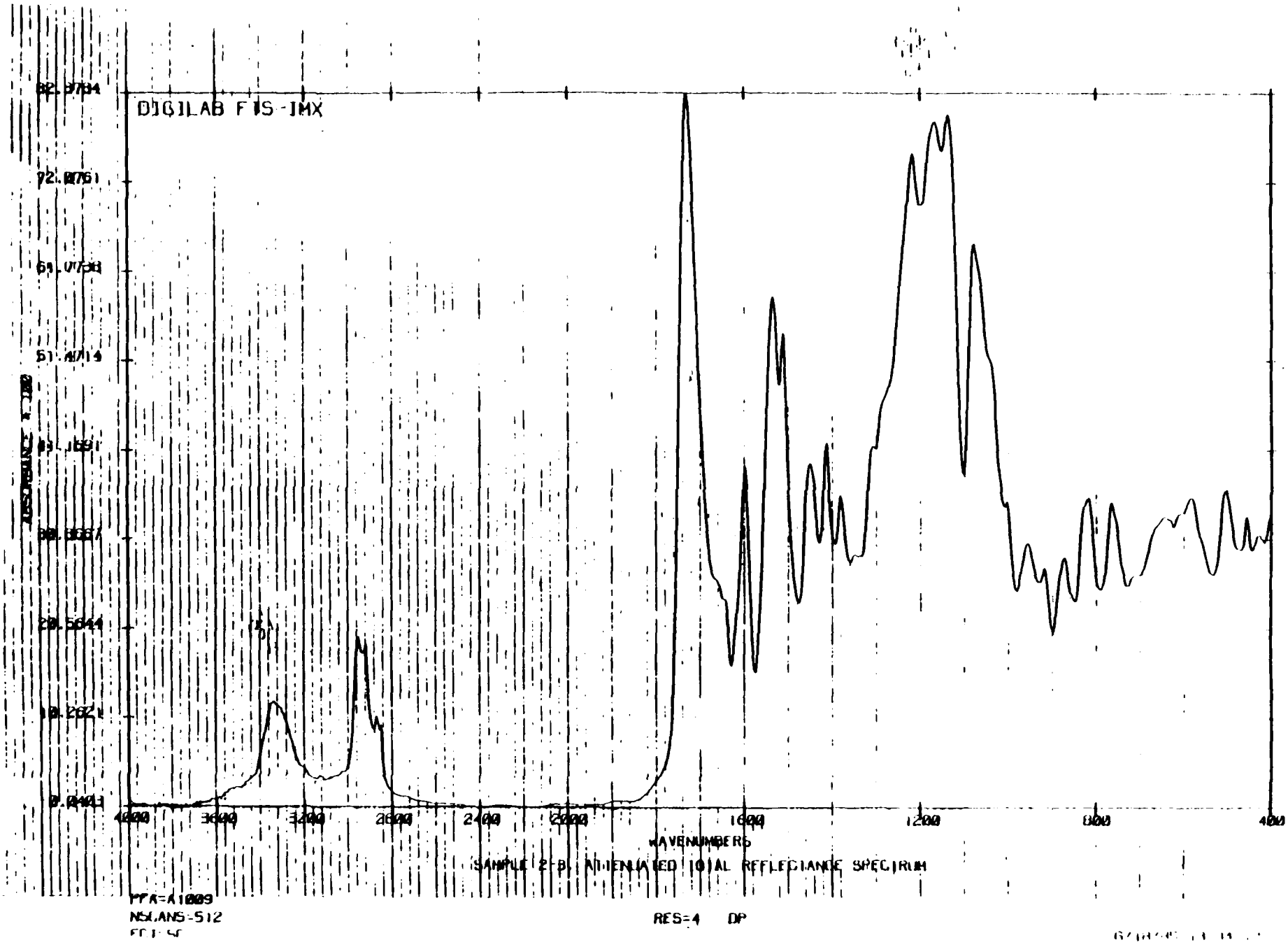
DIGILAB FTS-IMX
WAVENUMBERS
SAMPLE 2-B, ATTENUATED TOTAL REFLECTANCE SPECTRUM
PFA=A1009
NSCANS=512
RES=4 DP

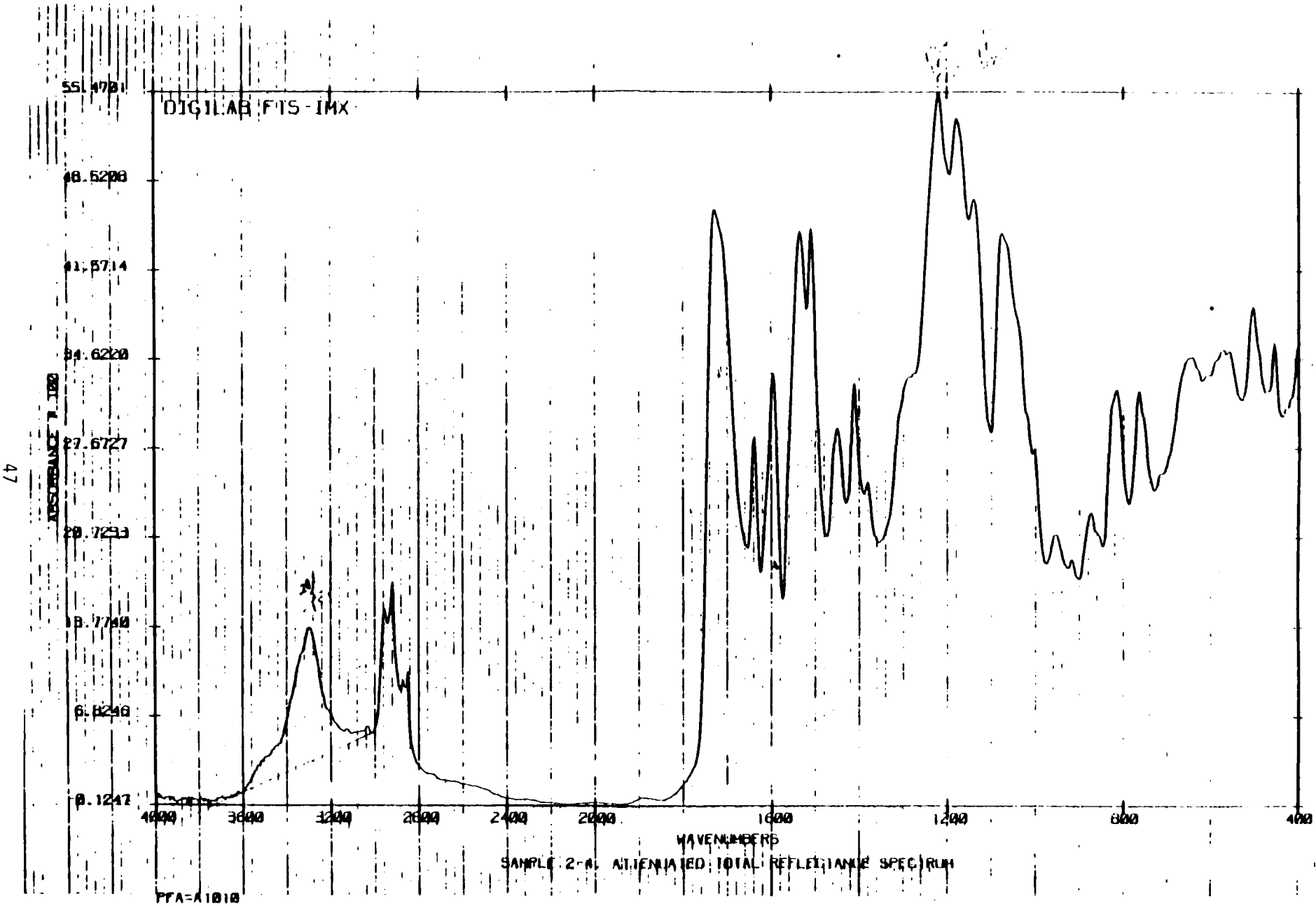
DIGILAB FTS-IMX
55.4701
48.6200
41.7714
34.9229
27.9727
21.2233
13.7740
6.8240
0.1247
ABSORBANCE
4000
3600
3200
2800
2400
2000
1600
1200
800
400
WAVENUMBERS
SAMPLE 2-A, ATTENUATED TOTAL REFLECTANCE SPECTRUM
PFA=A1010
NSCANS=512
RES=4 DP

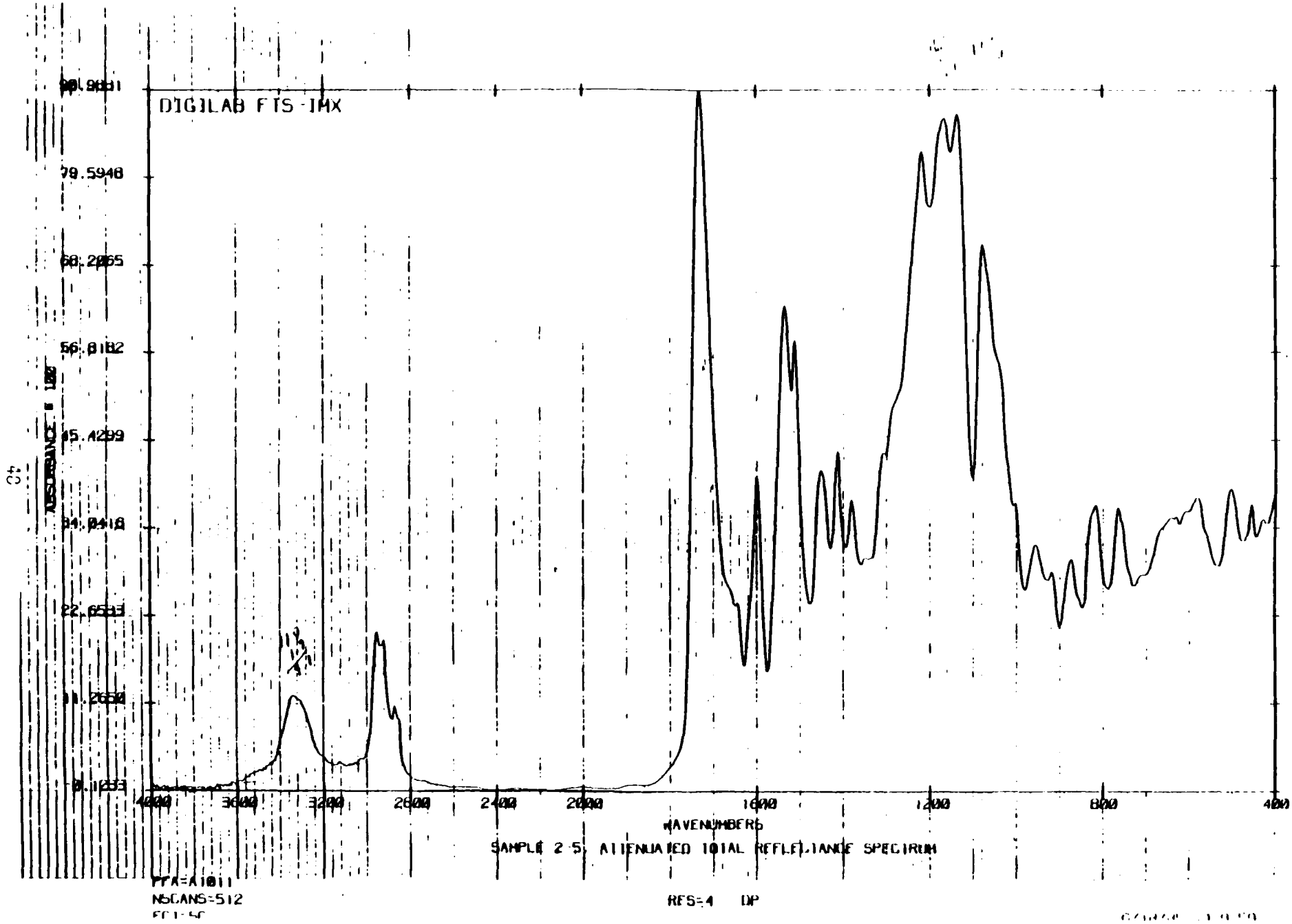
DIGILAB FTS-IMX
79.5948
68.2665
56.8182
45.4899
34.1618
22.8333
11.2650
4000
3600
3200
2800
2400
2000
1600
1200
800
400
WAVENUMBERS
SAMPLE 2-5, ATTENUATED TOTAL REFLECTANCE SPECTRUM
APR=A1011
NSCANS=512
RES=4 DP

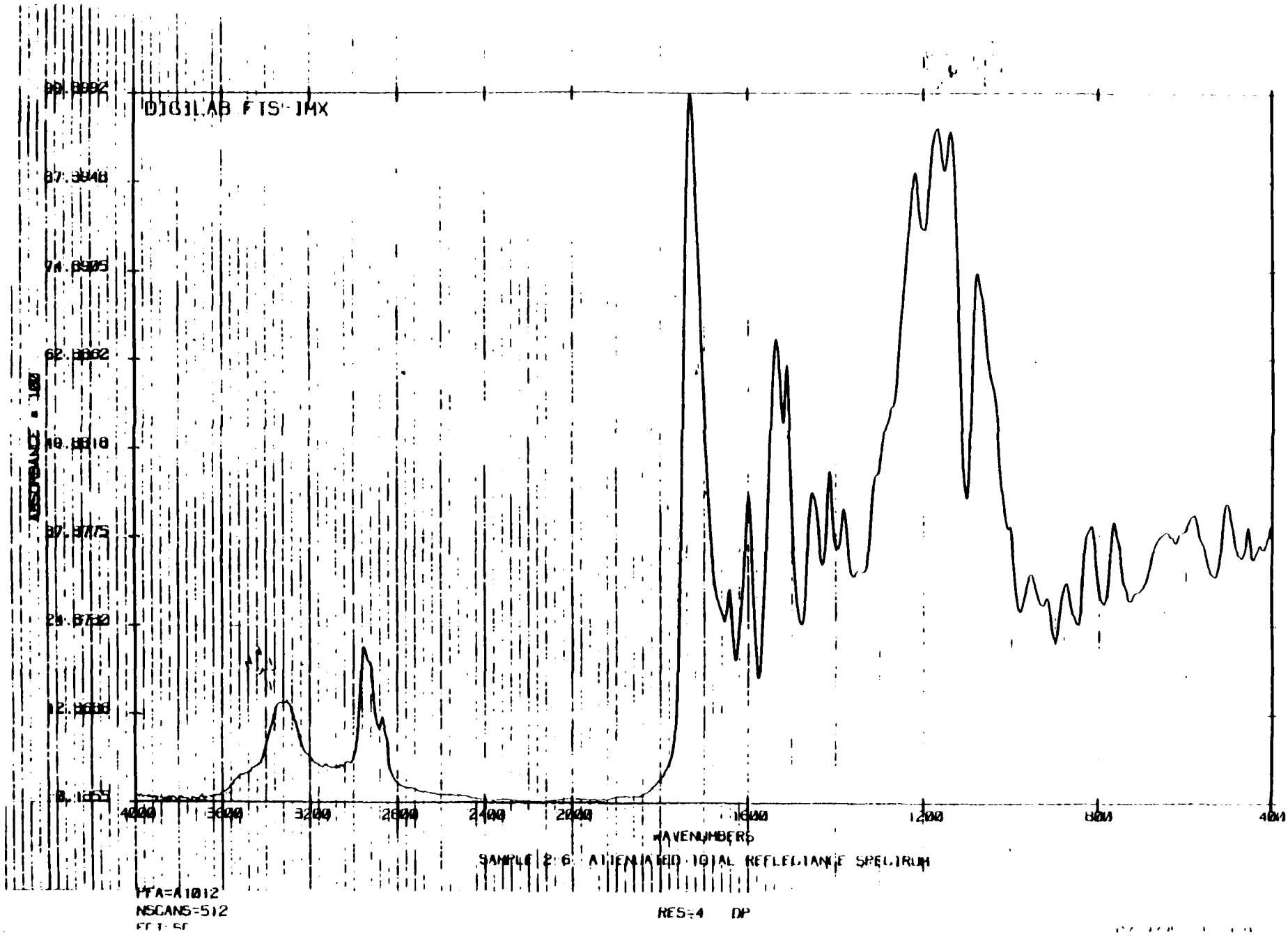
DIGILAB FTS-IHX
%REFLECTANCE
#WAVENUMBERS
SAMPLE 2:6 ATTENUATED TOTAL REFLECTANCE SPECTRUM
PFA=A1012
NSCANS=512
RES=4 DP

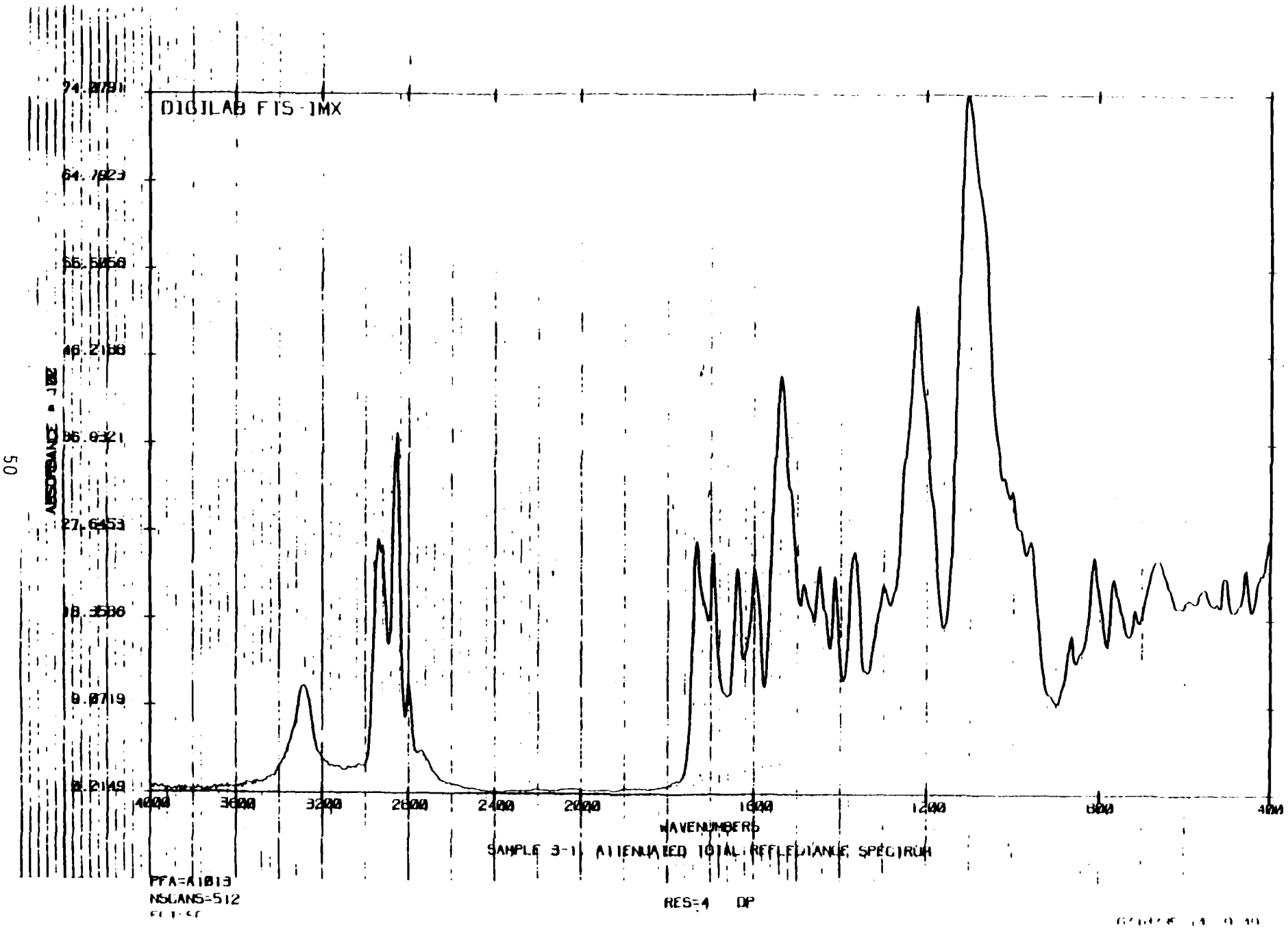
DIGILAB FTS-1MX
ABSORBANCE * 1000
64.1923
46.2138
36.0321
27.6453
18.3536
9.8719
2.2149
4000
3600
3200
2800
2400
2000
1600
1200
800
400
WAVENUMBERS
SAMPLE 3-1 ATTENUATED TOTAL REFLECTANCE SPECTRUM
PFA=A1B13
NSCANS=512
RES=4 DP

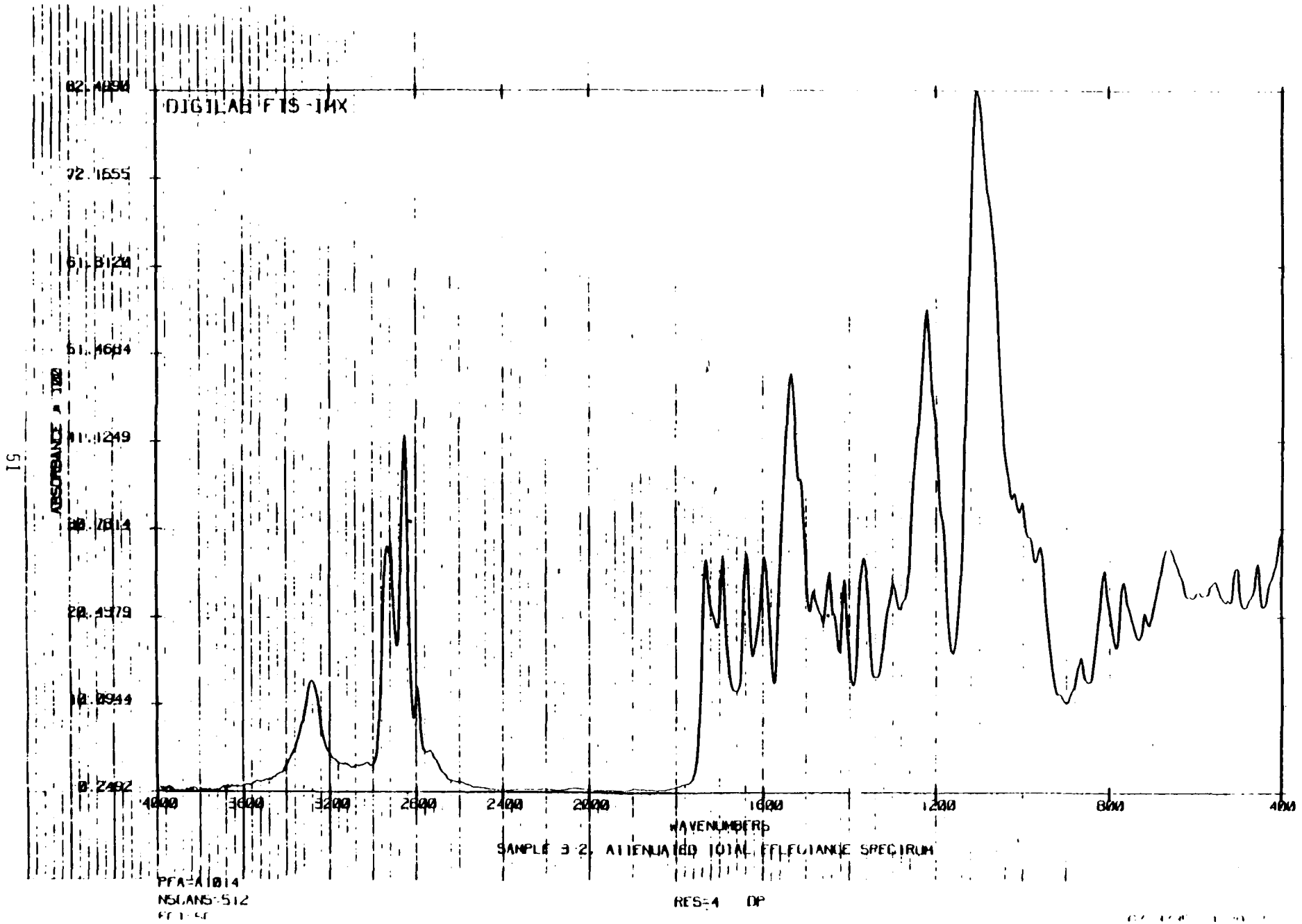
DIGILAB FTS-14X
72.1655
61.3124
51.4594
41.1249
30.7814
20.4379
10.0944
0.2492
ABSORBANCE * 100
4000
3600
3200
2800
2400
2000
1600
1200
800
400
WAVENUMBERS
SAMPLE 3 2. ATTENUATED TOTAL EFFECTANCE SPECTRUM
PFA=A1014
NSCANS=512
RES=4 DP

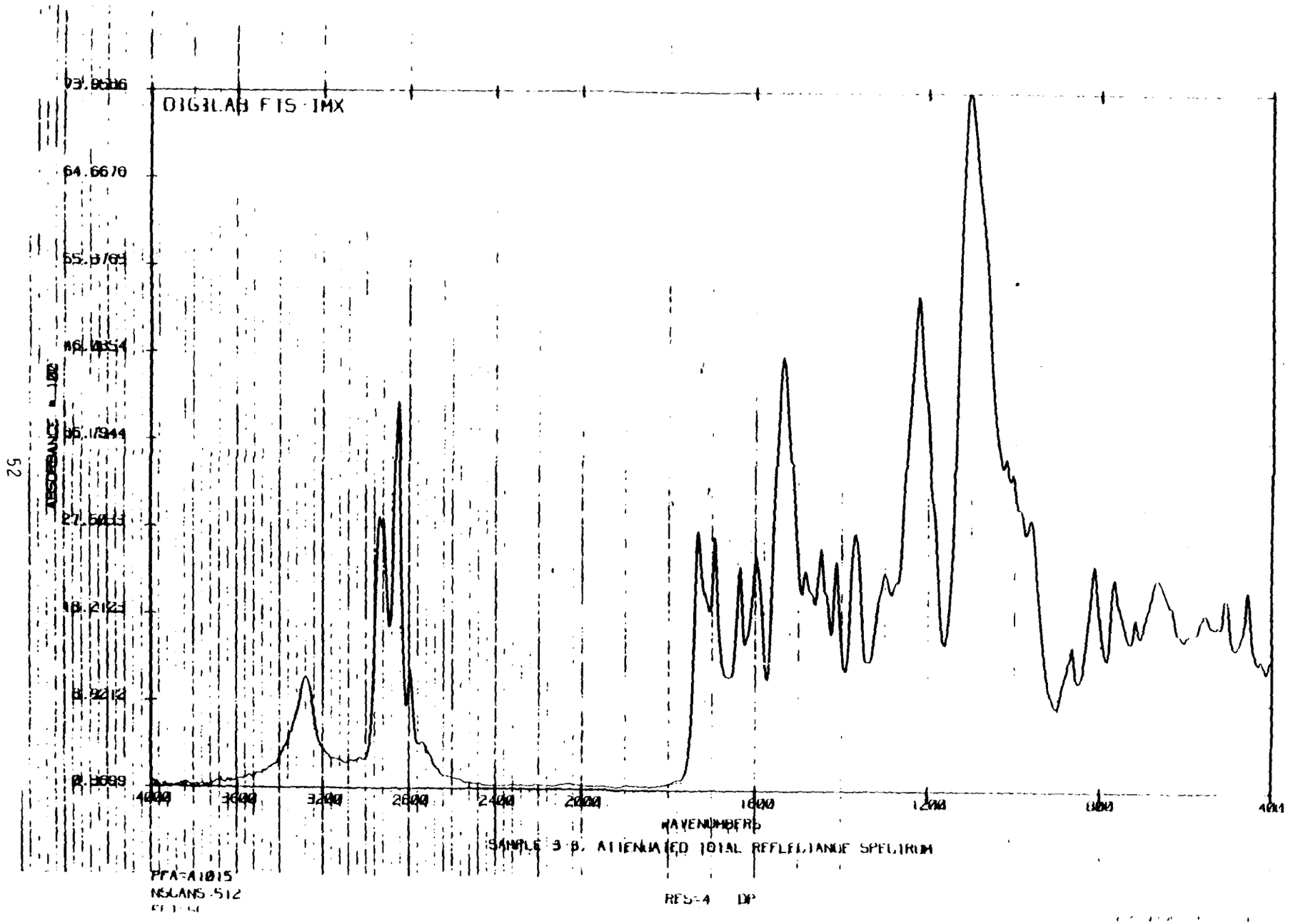
DIGILAB FTS-IMX
64.6670
ABSORBANCE
WAVENUMBERS
SAMPLE 3 β. ATTENUATED TOTAL REFLECTANCE SPECTRUM
PFA=A1015
NSCANS=512
RES=4 DP

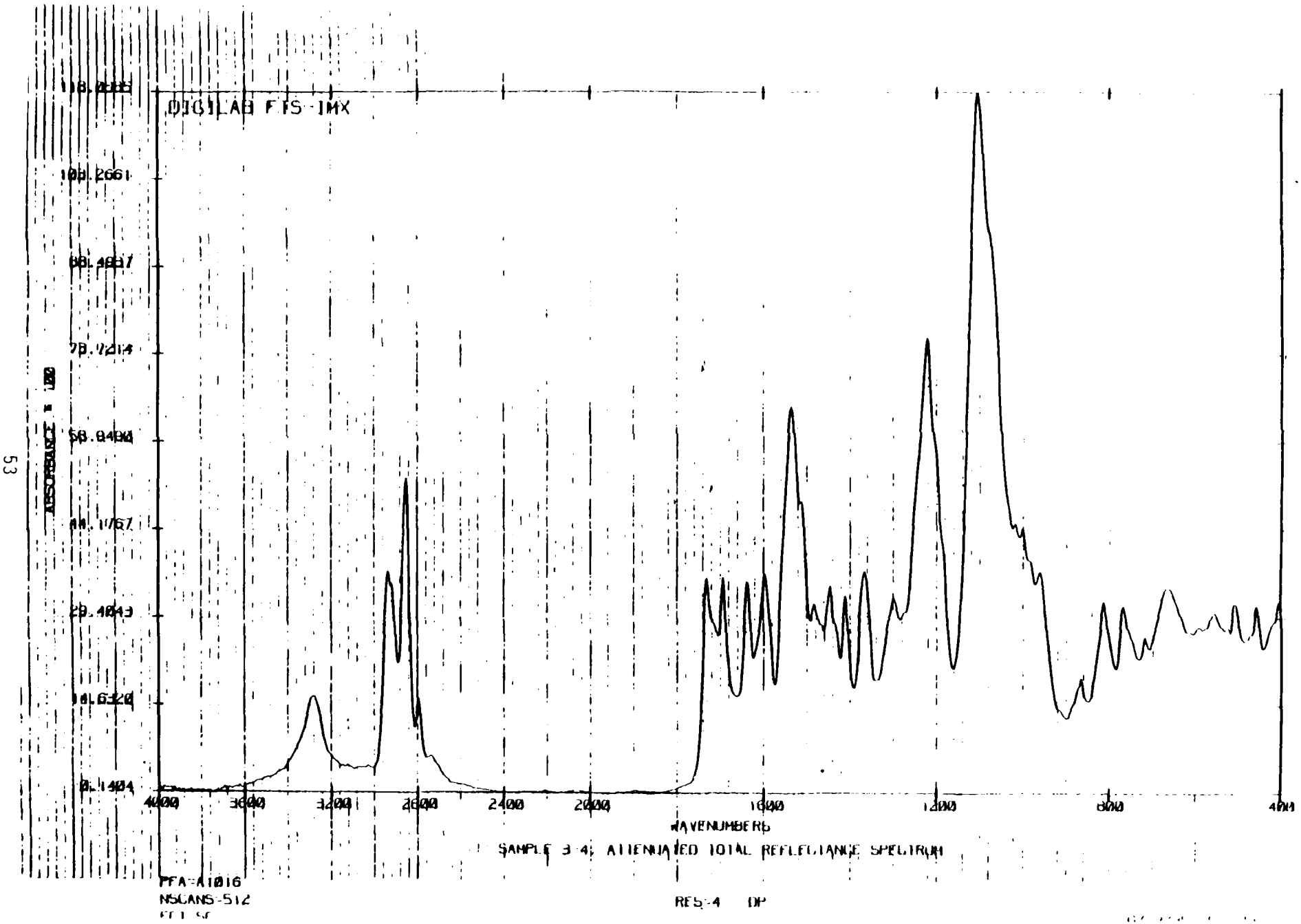
DIGILAB FTS-IMX
ABSORBANCE
WAVENUMBERS
SAMPLE 3-4; ATTENUATED TOTAL REFLECTANCE SPECTRUM
PFA-A1016
NSCANS-512
RES-4 DP

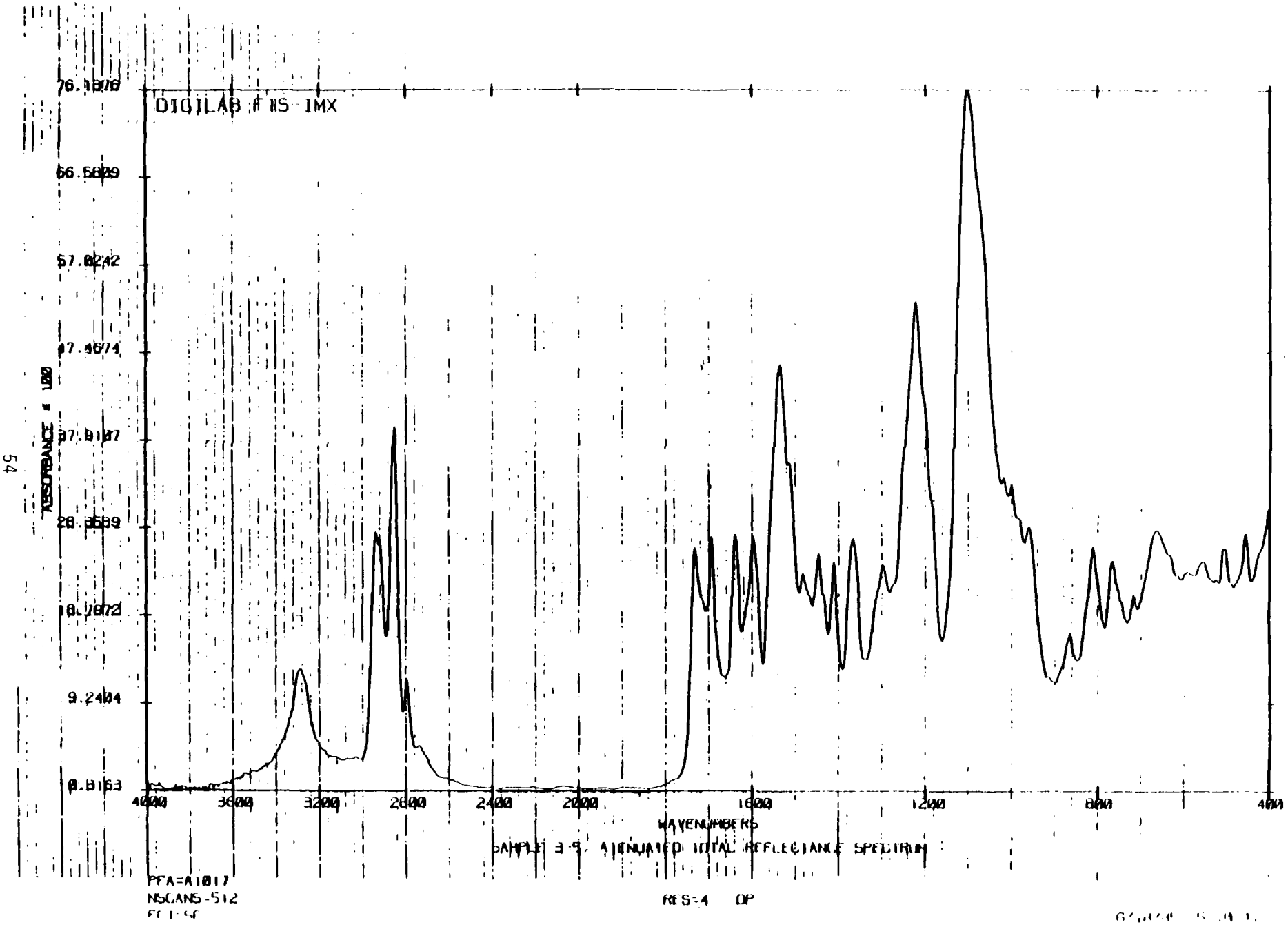
DIGILAB FTIS IMX
ABSORBANCE
66.5889
57.0242
47.4594
37.8947
28.3299
18.7652
9.2004
0.8153
4000
3600
3200
2800
2400
2000
1600
1200
800
400
WAVENUMBERS
SAMPLE 3-5, ALUMINED TOTAL REFLECTANCE SPECTRUM
PFA=A1017
NSCANS=512
RES=4 DP

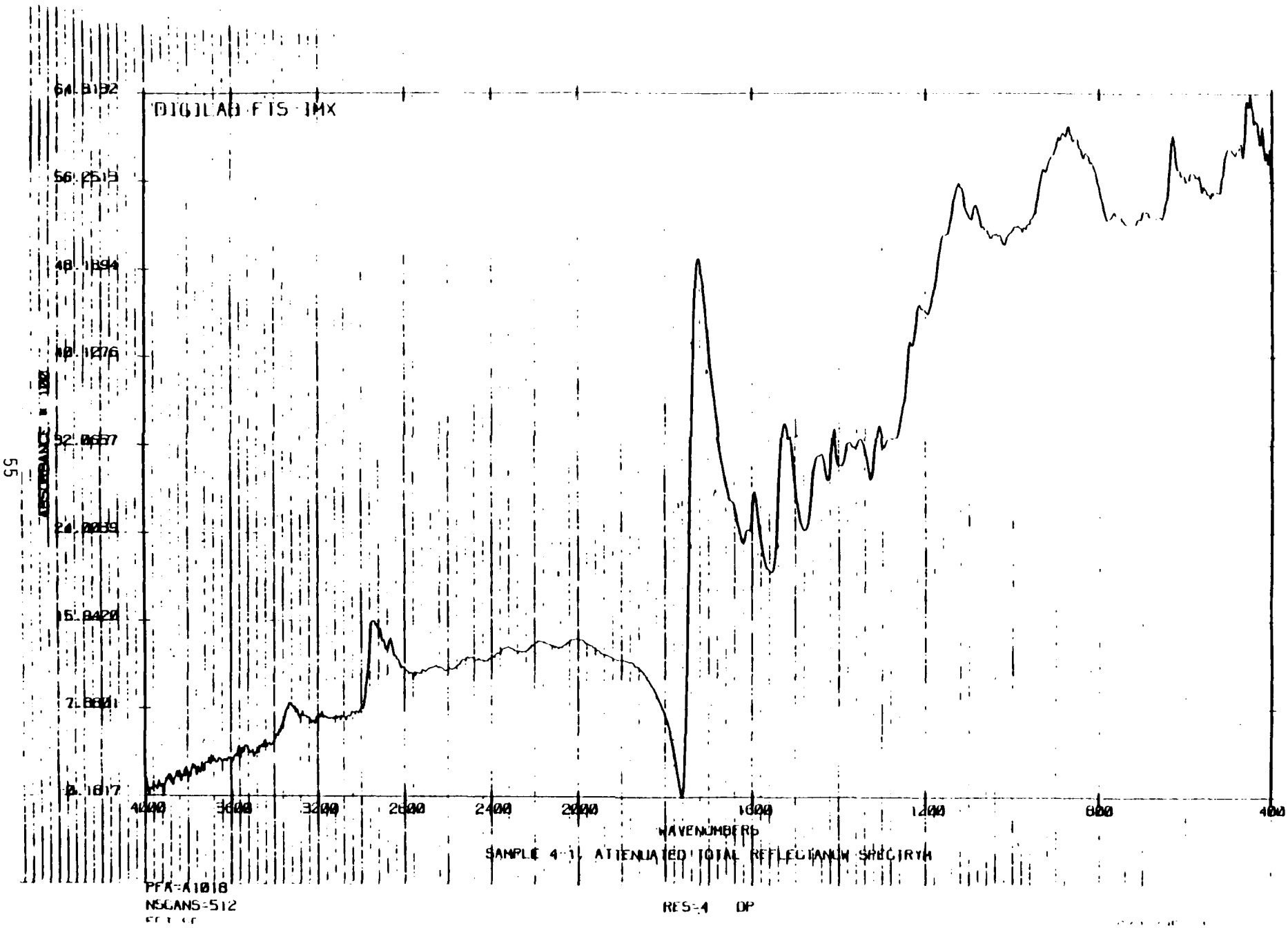
DIGILAB FTS IMX
WAVENUMBERS
SAMPLE 4-1, ATTENUATED TOTAL REFLECTANCE SPECTRA
PFA=A1018
NSCANS=512
RES=4 DP

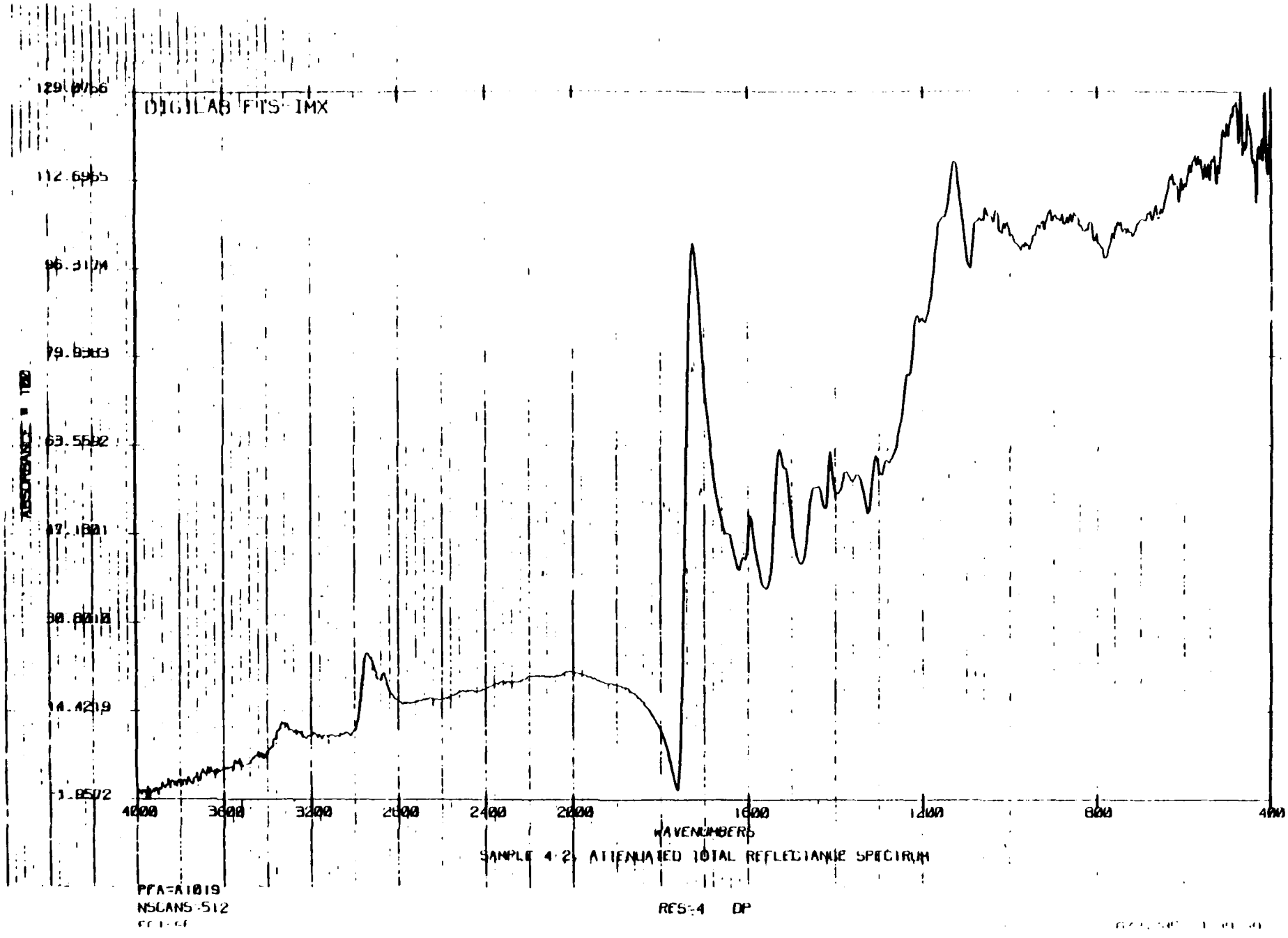
DIGILAB FTS IMX
ABSORBANCE
4000
3600
3200
2800
2400
2000
1600
1200
800
400
WAVENUMBERS
SAMPLE 4-2, ATTENUATED TOTAL REFLECTANCE SPECTRUM
PFA=A1019
NSCANS=512
RES=4 DP

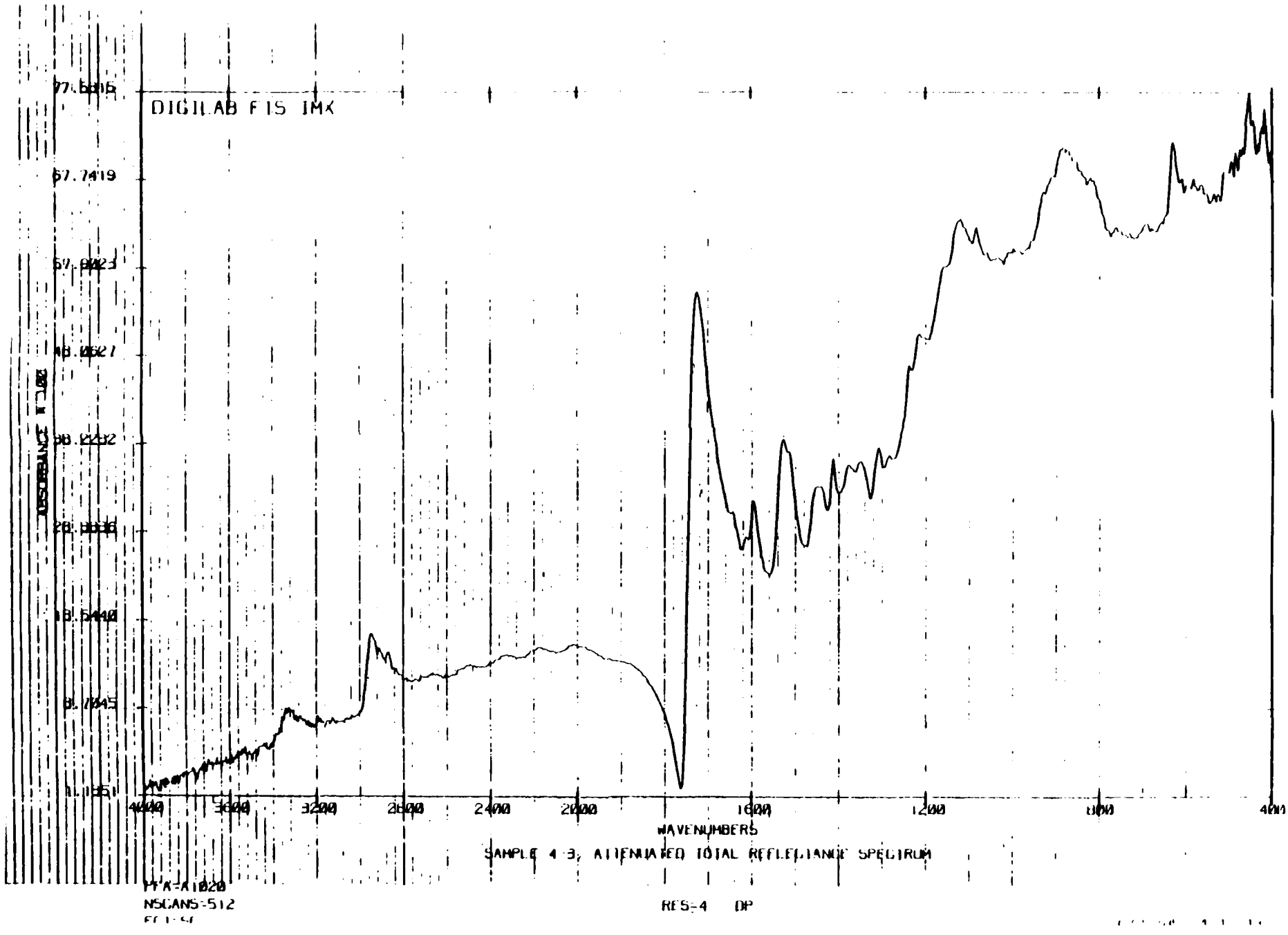
DIGILAB FTS IMX
WAVENUMBERS
SAMPLE 4-3, ATTENUATED TOTAL REFLECTANCE SPECTRUM
FTA=A1020
NSCANS=512
RES=4 DP

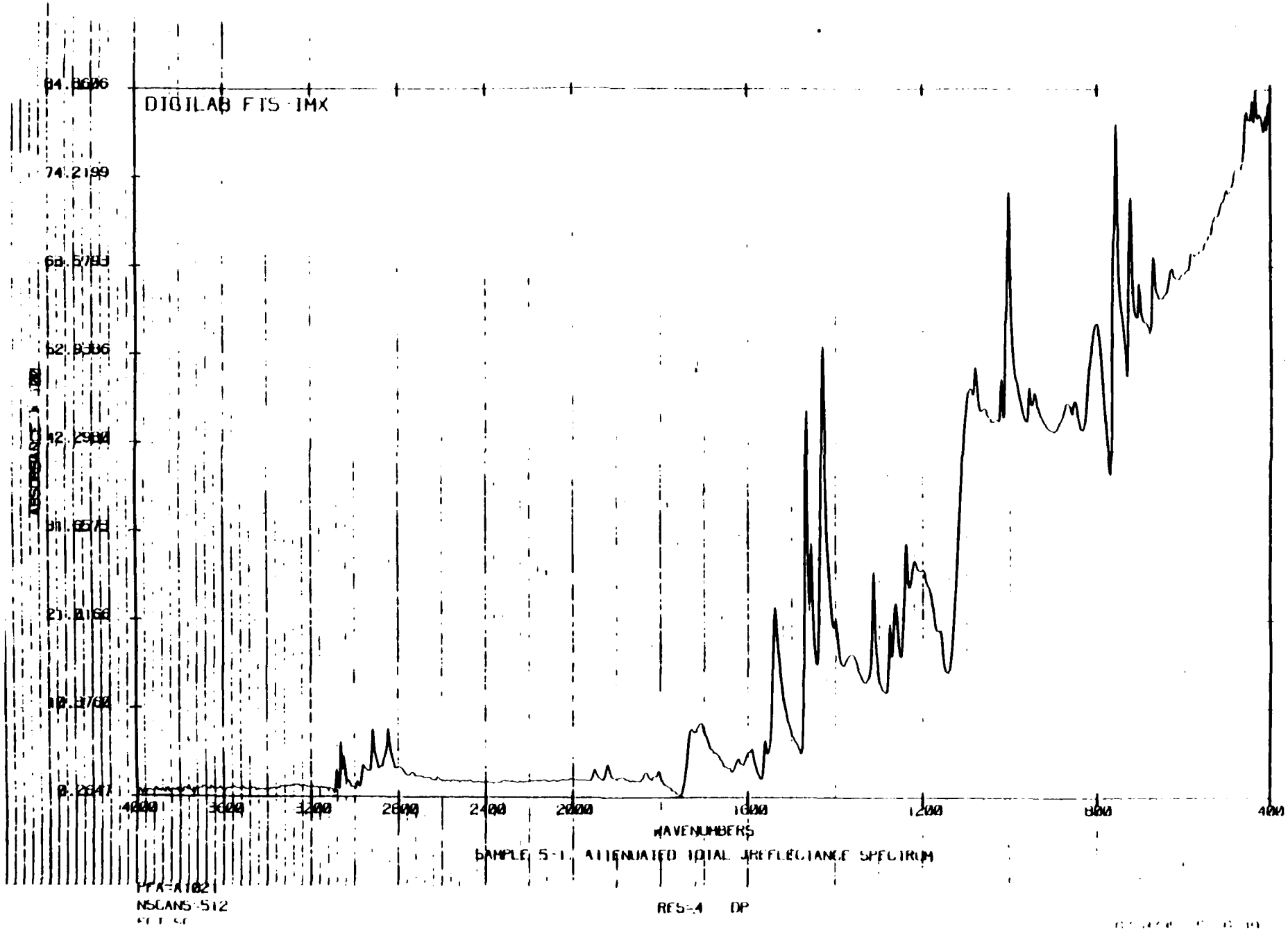
DIGILAB FTS-IMX
74.2199
42.2998
21.2168
WAVENUMBERS
SAMPLE 5-1, ATTENUATED TOTAL REFLECTANCE SPECTRUM
NSCANS=512
RES=4 DP

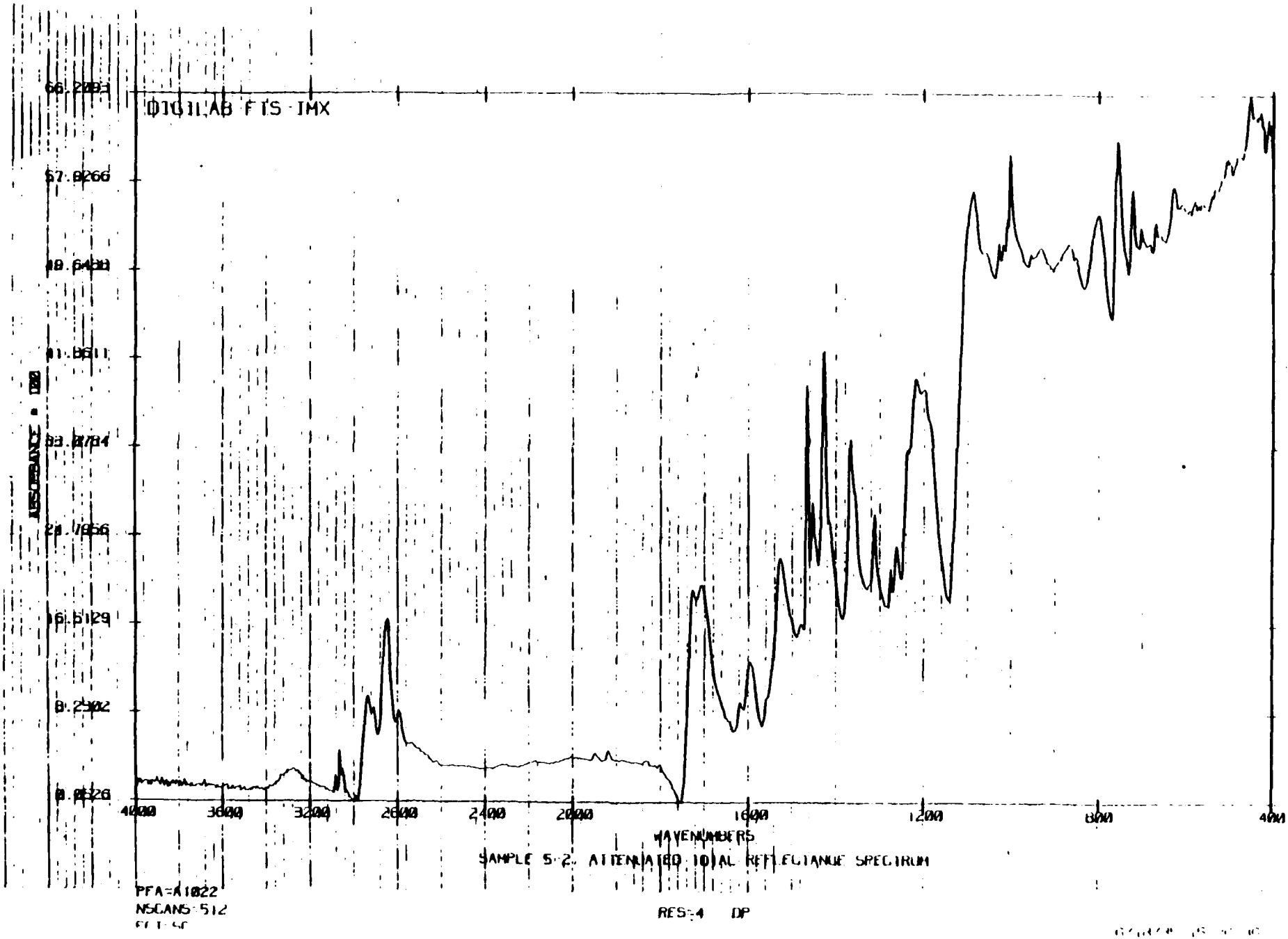
DIGILAB FTS-IMX
WAVENUMBERS
SAMPLE 5-2, ATTENUATED TOTAL REFLECTANCE SPECTRUM
PFA=A1022
NSCANS 512
RES=4 DP

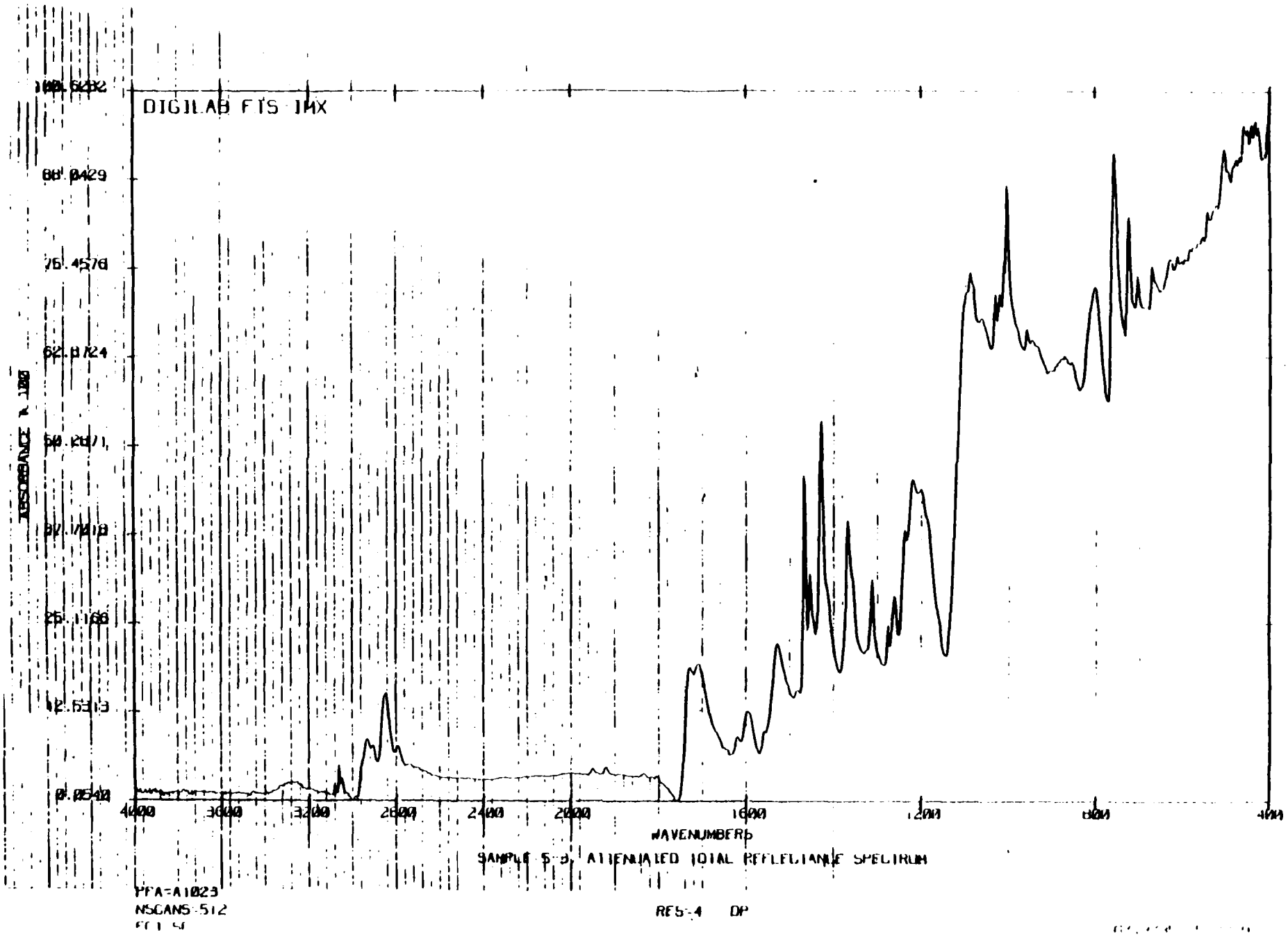

SAMPLE 5-3, ATTENUATED TOTAL REFLECTANCE SPECTRUM

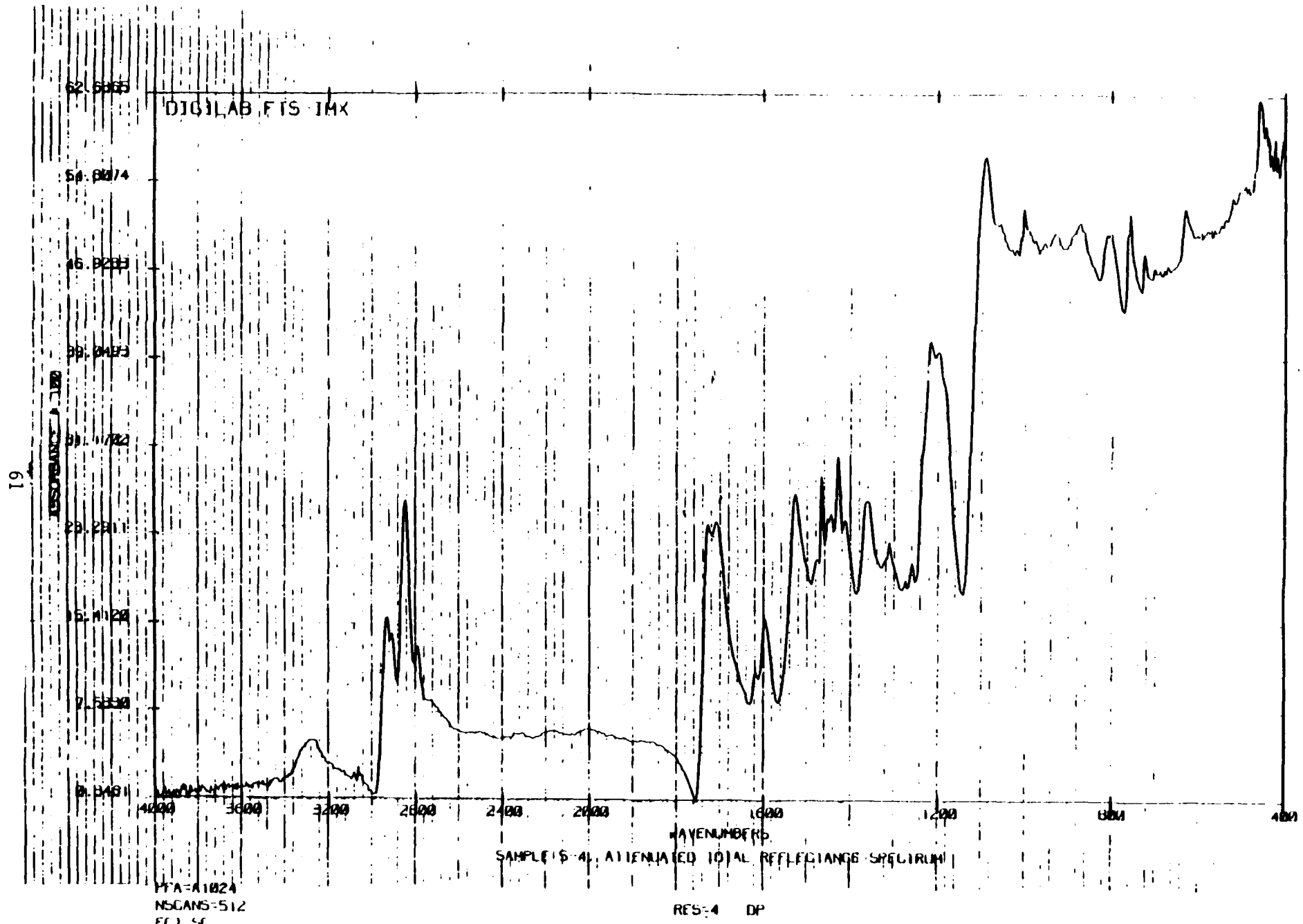
DIGILAB FTS IMX
ABSORBANCE
WAVENUMBERS
SAMPLE (S-4) ATTENUATED TOTAL REFLECTANCE SPECTRUM
PTA=A1024
NSCANS=512
RES=4 DP

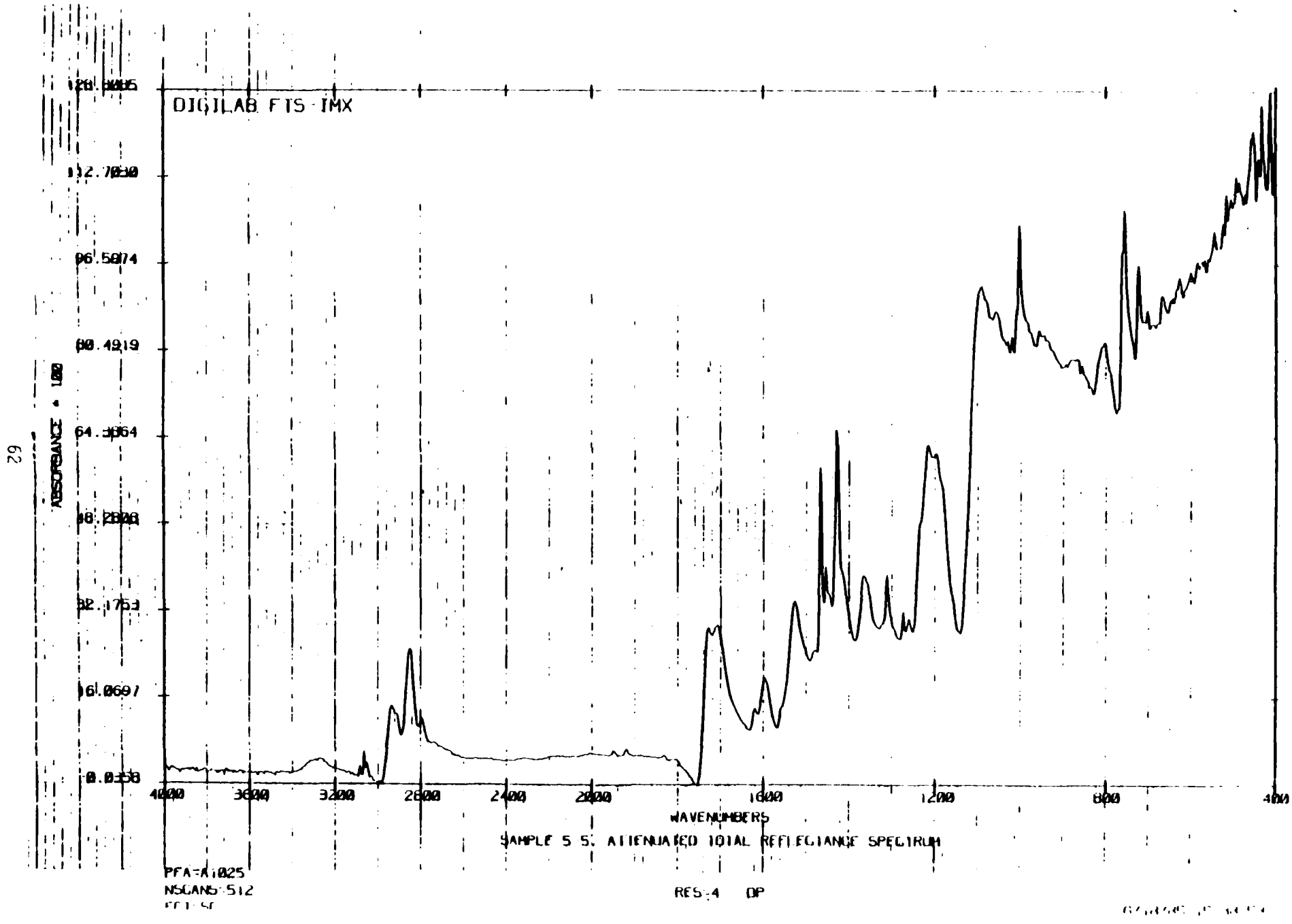
DIGILAB FTS-IMX
ABSORBANCE * 100
WAVENUMBERS
SAMPLE 5 5% ATTENUATED TOTAL REFLECTANCE SPECTRUM
PFA=A:025
NSCANS=512
RES=4 DP

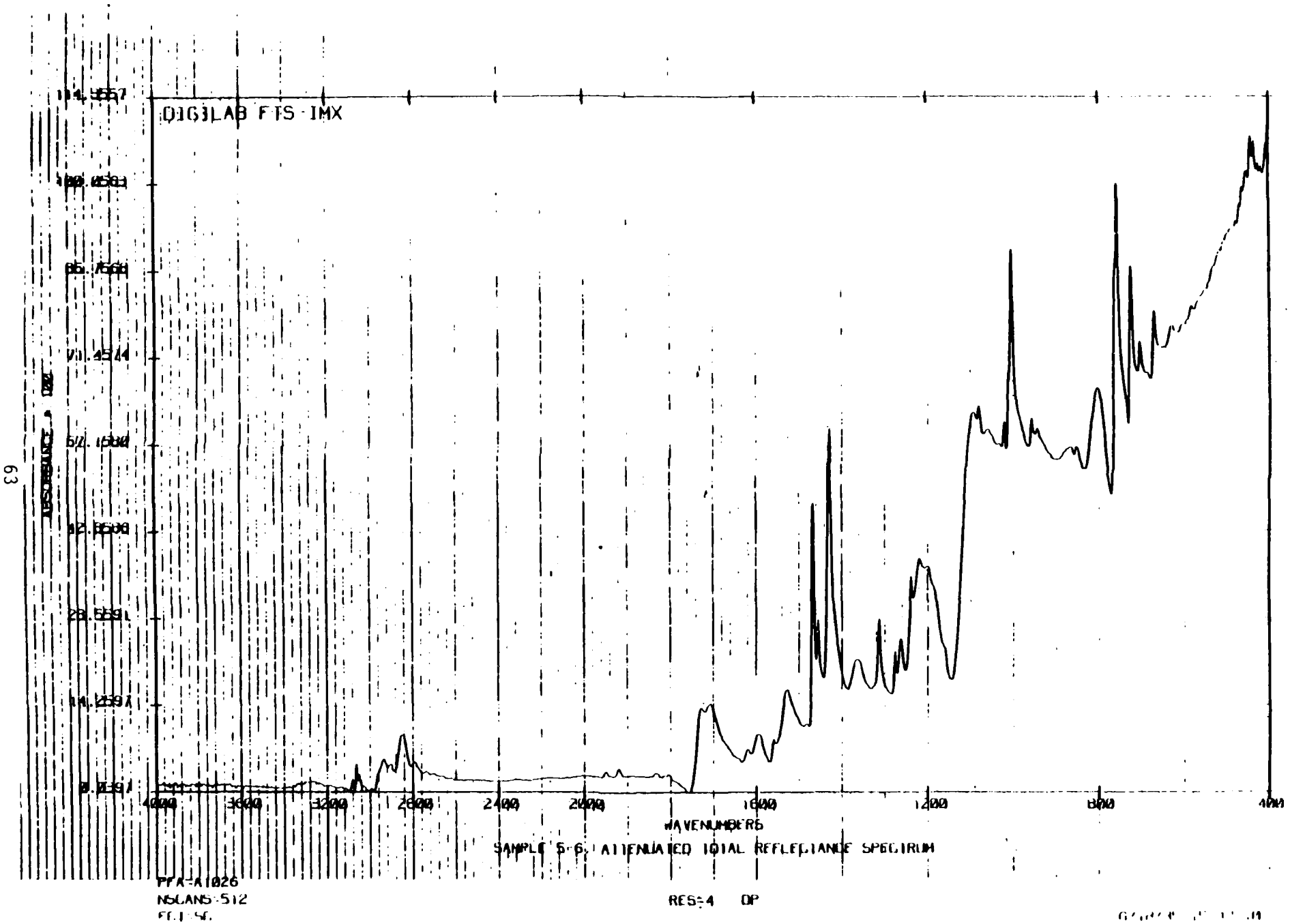
DIGILAB FTS-IMX
ABSORBANCE
WAVENUMBERS
SAMPLE 5-6, ATTENUATED TOTAL REFLECTANCE SPECTRUM
PFA-A1026
NSCANS-512
RES=4 DP

APPENDIX B

DESCRIPTION OF SwRI-DESIGNED INSTRUMENTS

DESCRIPTION OF INSTRUMENTS DESIGNED BY SwRI

1.0 Introduction

The purpose of the instruments described in the following paragraphs is to measure surface resistivity of the reinforced-polymer wall material of large flexible fuel tanks. Because this wall material is exposed to the weather and to sunlight, deterioration of the polymer constituents occurs, and there is evidence that surface resistivity of the wall material decreases as deterioration progresses; hence, it should be possible to determine degree of degradation by measuring this important surface property. However, surface leakage resistance of polymer materials is very high (on the order of thousands of megaohms), which means that conventional ohmmeter techniques are not applicable. Special consideration must be given to keeping stray shunt resistances in the metering circuits higher than the resistance to be measured. This is accomplished by using very high-grade dielectric materials (such as Teflon), special input devices (e.g., MOS field-effect transistors of electrometer tubes) in the electronic measuring circuits, and guarding techniques.

Conventional high-resistance leakage meters generally apply a potential on the order of a few hundred volts across the specimen to be measured to minimize measuring circuit input-resistance problems; however, in the case of measuring fuel-tank-wall surface resistance, there is a high probability that flammable fuel vapors will be present in the measurement area, so presence of a power supply capable of delivering several hundred volts represents a potential safety hazard. This problem can be minimized by using low voltages in the measuring instrument, and this specific consideration is the primary driving force behind designing a special-purpose low-voltage high-resistance leakage meter.

There are two principles that may be employed in the design of a high-resistance leakage meter. These principles are based upon capacitance-charging and voltage dividing. The capacitance charging principle was

employed during the course of this study and is discussed in detail. The voltage divider principle was not used due to unavailability of parts but is potentially the better system and therefore, is discussed.

The first approach for which components are readily available off-the-shelf is to charge a small capacitance through the unknown resistance and to determine the time required for charge to grow to a predefined fraction (typically 50%) of the maximum available charged. Chief disadvantage of this instrument is that the specimen is not at ground potential which complicates the experimental procedure and introduces a number of stray parameters that cannot be readily determined or compensated; hence, an instrument employing this principle cannot be expected to yield accurate and reliable results. However, under laboratory conditions and with procedural care, approximate results, suitable for establishing general trends, may be obtained.

The second type of meter designed at SwRI is based upon a voltage-divider principle of operation. Some of the parts have too long of a delivery time and, therefore, this meter will not be built during this program. It is discussed in this report because we feel it definitely warrants future investigation. This second and best approach from the standpoint of simplicity, accuracy and stability is to place the unknown specimen in the lower arm of a resistive voltage divider that is supplied from a constant-voltage source and to measure the fraction of the applied voltage that appears across the unknown resistance. To make this system work, the top resistor in the voltage divider must be of the same order of magnitude as the unknown resistance; hence, resistance values in the range of 10^{10} to 10^{14} ohms may be required. Such resistors are not available off-the-shelf and, therefore, must be custom-made; delivery time for these resistors has been quoted at 8 to 10 weeks. Advantages of the voltage-divider system are that the unknown resistance is effectively compared with a known resistance (i.e., the resistor in the upper arm of the voltage divider) and the unknown resistor is at ground potential which simplifies experimental procedure.

Both instruments require a probe which defines the resistance being measured. A coaxial probe arrangement is used so that the unknown is in the

form of an annulus. In using this configuration with an instrument employing the voltage-divider principle, the outer electrode of the probe is at ground potential which greatly simplifies handling and measurement procedures. In the capacitance instrument, however, the external electrode of the probe is elevated above ground potential which effectively limits use of this instrument to the laboratory; further because stray capacitances affect the measurement result in the capacitance instrument, a significantly different probe design is required.

We have fabricated an instrument employing the capacitance-charging technique so that some preliminary laboratory data can be acquired in the near future and to fabricate a voltage-divider instrument at a later time, perhaps on a subsequent contract. As mentioned above, the capacitance-charging instrument is suitable only for laboratory use and for obtaining approximate results. Additionally, because known high-resistance resistors (i.e., the long-delivery items) were not available within a suitable time frame, it is not possible to calibrate the capacitance-charging instrument in absolute resistance terms; accordingly, readings obtained from this instrument are only relative.

2.0 Capacitance Changing

Basic approach to high-resistance measurement incorporated in the described instrument is charging a capacitance through the unknown resistance and determining time required for charge to grow to a predefined fraction (typically 50%) of the maximum available. The chief disadvantage of this instrument is that the specimen is not at ground potential which complicates experimental procedure and introduces a number of stray parameters that cannot be readily determined or compensated; hence, an instrument employing this principle cannot be expected to yield accurate and reliable results. However, under laboratory conditions and with procedural care, approximate results, suitable for establishing general trends, may be obtained.

The instrument includes a switch to select various capacitors so that a broad range of resistance values can be accommodated. A power supply in the instrument provides the potential source for charging the range capacitors,

and a high-input-resistance electronic amplifier transforms the voltage developed across the capacitor into an equivalent voltage available at low impedance. Output of this amplifier drives a guard circuit which minimizes effects of stray leakage.

Output of the electronic amplifier in the capacitance-charging instrument is also fed to a voltage comparator which is set to switch at a predetermined fraction (i.e., 50%) of the maximum available charging voltage. When this threshold is reached, a free-running digital counter is stopped, and the final count value is displayed on a digital readout.

2.1 Detailed Circuit Description

The instrument is divided into four sections related principally to location in the package. There are three printed-circuit boards, which include the analog, digital and display boards, and the chassis-mounted components, which include the range switch, read button, batteries, power supply, etc. The following circuit descriptions include the chassis-mounted components most closely associated with the particular circuit being discussed; there is no separate discussion of the chassis-mounted components themselves.

2.1.1 Analog Circuit

The analog circuit and associated chassis-mounted components are connected as shown in the schematic diagram of Figure 1. Key components in the analog circuit include zener diode CR1 which supplies a constant reference voltage to the UNKNOWN and to the voltage comparator U2. Switch s1 is the RANGE switch which selects a particular charging capacitor appropriate for the resistance being measured; capacitors C2 through C7 are the range capacitors which are charged through the unknown leakage resistance. Switch S2A is the READ pushbutton which controls the measurement cycle. Metal-oxide-silicone field-effect transistor (MOSFET) Q1 is connected as a source follower which provides a high input impedance suitable for interfacing with the high resistance input circuits and a relatively low output impedance suitable for driving subsequent circuitry. Resistors R6 and R7 and capacitors C8 and C9

form a low-pass filter intended to reject power-line interference that may be picked up in the high-impedance input circuits. Operational amplifier U1, connected as a noninverting amplifier, has enough gain to compensate for the source-follower loss; thus, net voltage gain from the gate of MOSFET Q1 through the output of operational amplifier U2 is unity. Output of operational amplifier U1 feeds the inverting input of voltage comparator U2, output of which is routed to the digital circuits discussed later.

In operation, the unknown (i.e., a carefully defined area of polymer fuel-tank wall material) is connected between the two UNKNOWN terminals using stiff open wires. Range switch S1 is used to select a range capacitor, following which the read button S2A is depressed, then released. Depressing the pushbutton discharges the selected range capacitor, and through a ganged switch S2B (to be discussed later), resets and arms a 4-digit counter on the digital circuit board. When the READ button is released, the small leakage current flowing through the unknown is accumulated on the selected range capacitor, and voltage across that capacitor increases almost linearly as a function of time. Voltage developed across the selected range capacitor is transferred by the unity-gain amplifier comprising MOSFET Q1 and operational amplifier U1 to the inverting input of voltage comparator U2. The noninverting input of voltage comparator U2 is held at a potential equal to approximately 50% of the reference voltage set by zener diode CR1. When the voltage developed across the selected range capacitor reaches the voltage-comparator threshold, output of the comparator suddenly changes logic state (i.e., goes from logic 1 to logic 0), and this transition triggers responses in the digital circuits to be discussed later.

Output of operational amplifier U1 serves an additional purpose by providing a guard potential to electrical conductors that surround, but are insulated from, critical high-impedance input circuits associated with the UNKNOWN. By making the potential difference between (1) conductors actually connected to the UNKNOWN and (2) surrounding guard conductors equal to zero, there can be no current flow between the guarded and guarding conductors; hence, stray shunt resistances (e.g., leakage resistances of printed-circuit board material, switch components, feed through insulators, etc.) can be reduced to zero so that they do not interfere with the minute leakage current flowing through the unknown specimen.

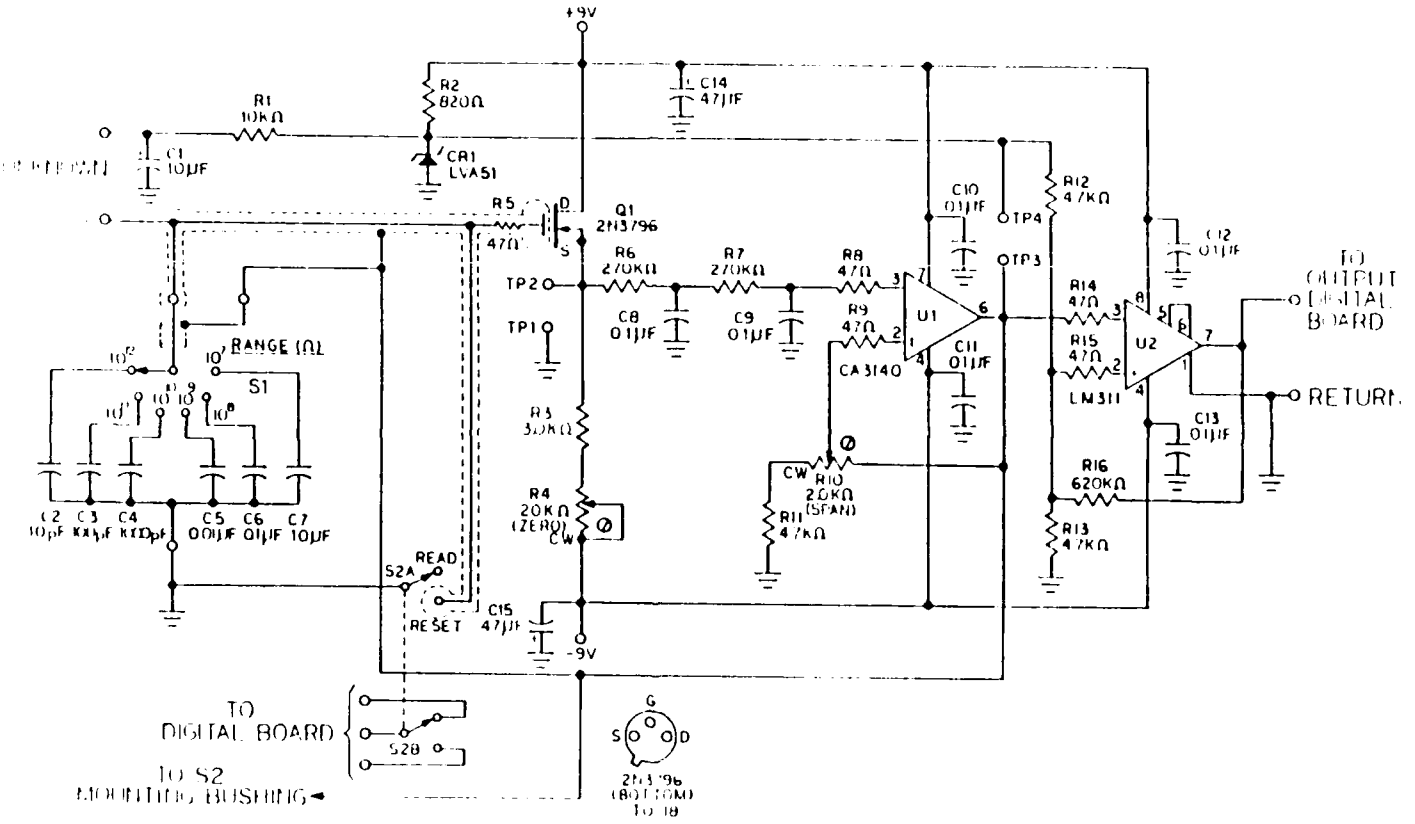

Figure 1. Schematic Diagram of Analog Board

2.1.2 Digital Circuit

Principal elements of the digital circuit, comprising a free-running multivibrator, a four-digital binary-coded-decimal (BCD) counter, a digital display and control circuits, are connected as shown in Figure 2. Timer U21 is used as a free-running multivibrator which generates a 100-Hz pulse train having approximately 10% duty cycle. Output of this multivibrator, by way of control circuitry, provides the clock-pulse input to the four-digit counter.

Decade counters U24 through U27 form the four-digit BCD counter. The most-significant-digit (MSD) output of each counter stage feeds the clock input of the subsequent stage such that any given stage in the counter advances one count whenever the preceding stage has accumulated then input counts. BCD-to-7-segment decoders U28 through U31 function as interfaces between BCD outputs of the individual counter stages and 7-segment digital displays U34 through U37.

Integrated circuits U22, U23, U32 and U33 control operation of the four-digit counter. Specifically, NAND gate U22A is the principal controlling element for the counter. When conditions are correct, clock pulses from free-running multivibrator U21 pass through NAND gate U22A to the clock input of the least-significant-digit (LSD) counter stage U24. NAND gates U23A and U23B are connected as a set-reset flip-flop which is used as a contact debouncer for the READ switch S2B. When this switch is in the "Read" (i.e., normal) position, an enabling input is delivered to NAND gate U22A. However, when the READ switch is depressed (i.e., the "Reset" condition), the flip-flop formed by U23A and U23B changes state such that four actions occur: (1) a disabling signal is delivered to NAND gate U22A, (2) the flip-flop formed by U23C is set thus sending an enabling logic signal to NAND gate U22A, (3) flip-flop U32A is reset (action of this flip-flop will be discussed later) and (4) the four counter stages are reset to zero. As previously mentioned, depressing the READ switch also discharges the range capacitor in the analog section, and this has the ultimate effect of causing output of voltage comparator U2 to transfer to the high logic stage which, in turn, prepares the flip-flop formed by NAND gates U23C and U23D to accept a future input. When the READ

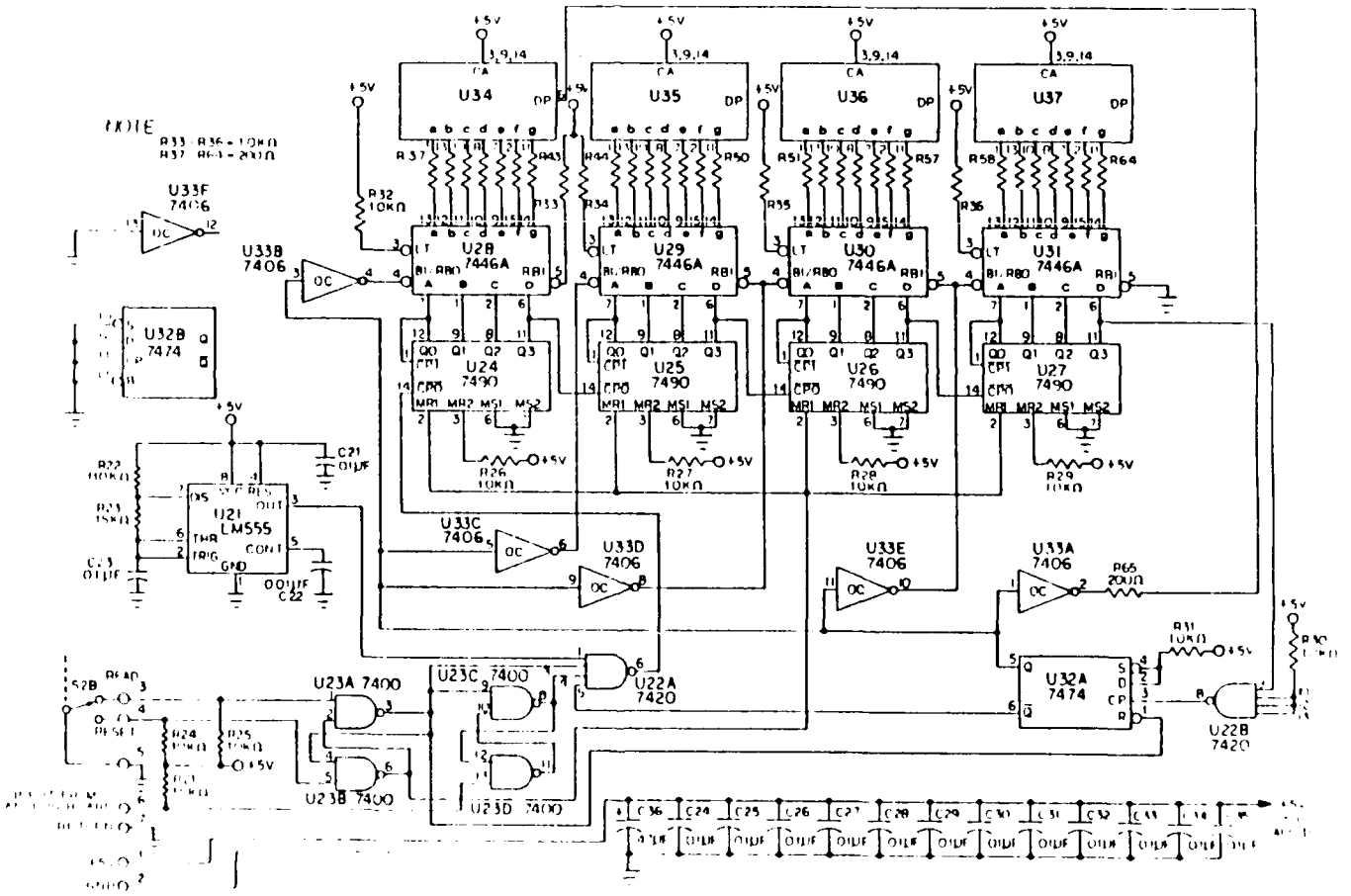

Figure 2. Schematic Diagram of Digital Board

pushbutton is released so that it returns to the "Read" position, output of the flip-flop formed by NAND gates U23A and U23B changes state and, consequently, counter stages U24 through U27, flip-flop U32A and the flip-flop formed by NAND gates U23C and U23D are all enabled. In addition, the final enabling signal is sent to NAND gate U22A which begins passing clock pulses from multivibrator U21 to the first stage U24 of the four-digit counter.

While the system is in this transitory state, the counter operates until one of two conditions occurs; the first (normal) condition is that voltage developed across the selected range capacitor passes through the voltage comparator threshold, in which case output of voltage comparator U2 falls to logic level zero. This action resets the flip-flop formed by NAND U23C and U23D which, in turn, delivers a disabling signal to NAND gate U22A, thereby interrupting clock pulses to the four-digit counter and terminating the count. At this point, the digital display indicates the total count accumulated in the four-digit counter. While this count is not linearly proportional to leakage resistance of the unknown specimen, it does correlate with the unknown resistance according to a consistent relationship; hence, readings obtained with this instrument must be considered relative in nature.

If the selected range capacitor is too large, the alternate count-termination system takes effect; that is, if the count exceeds 9999 before voltage developed across the range capacitor reaches the 50% threshold, a logic transition is fed to the clock input of flip-flop U32A by way of inverter-connected NAND gate U22B. This transition causes flip-flop U32A to change state and send a disabling signal to NAND gate U22A, thereby cutting OFF clock pulses to the counter. Further, the digital display is blanked and the decimal point in the most-significant digit of the display is illuminated. Thus, when a blank display with a single decimal point illuminated is observed, it means that the unknown resistance is higher than the selected range can accommodate; it is then necessary to choose a smaller range capacitor (i.e., a higher resistance range) and reinitiate the measurement process. As noted earlier, depressing the read pushbutton resets flip-flop U32A, thereby restoring the display and turning off the decimal point overrange indicator.

2.1.3 Other Circuits

Other circuits in the instrument include two 9-volt transistor-radio batteries which supply the analog circuits and a double-pole POWER switch for these batteries. Additionally, there is a line-powered 5-V supply for the digital circuits and a separate POWER switch for this supply. Connections of these components are detailed in Figure 3. Thus, to turn the instrument on or off, it is necessary to operate two POWER switches.

2.2 Adjusting Procedure

Under normal laboratory operating conditions for which this instrument was designed, the two analog adjustments should be stable. Operation of the circuit can be checked by the following procedure and adjustments can be made if necessary.

(1) Move both POWER switches to their OF positions and disconnect line cord from POWER source.

(2) Remove four screws that hold front panel in place, and fold front panel forward and down.

(3) Connect a floating (i.e., ungrounded) dc voltmeter (1-V scale) between test points TP1 and TP2 on the analog circuit board.

(4) Move the BATTERY POWER switch to the ON position.

(5) While holding the READ switch in the depressed position, adjust trimmer potentiometer R4 on the analog circuit board to produce a voltmeter reading of D V. When this adjustment is complete, release the READ pushbutton.

(6) Reconnect the floating (i.e., ungrounded) dc voltmeter (1-V scale) between test points TP3 and TP4 on the analog circuit board.

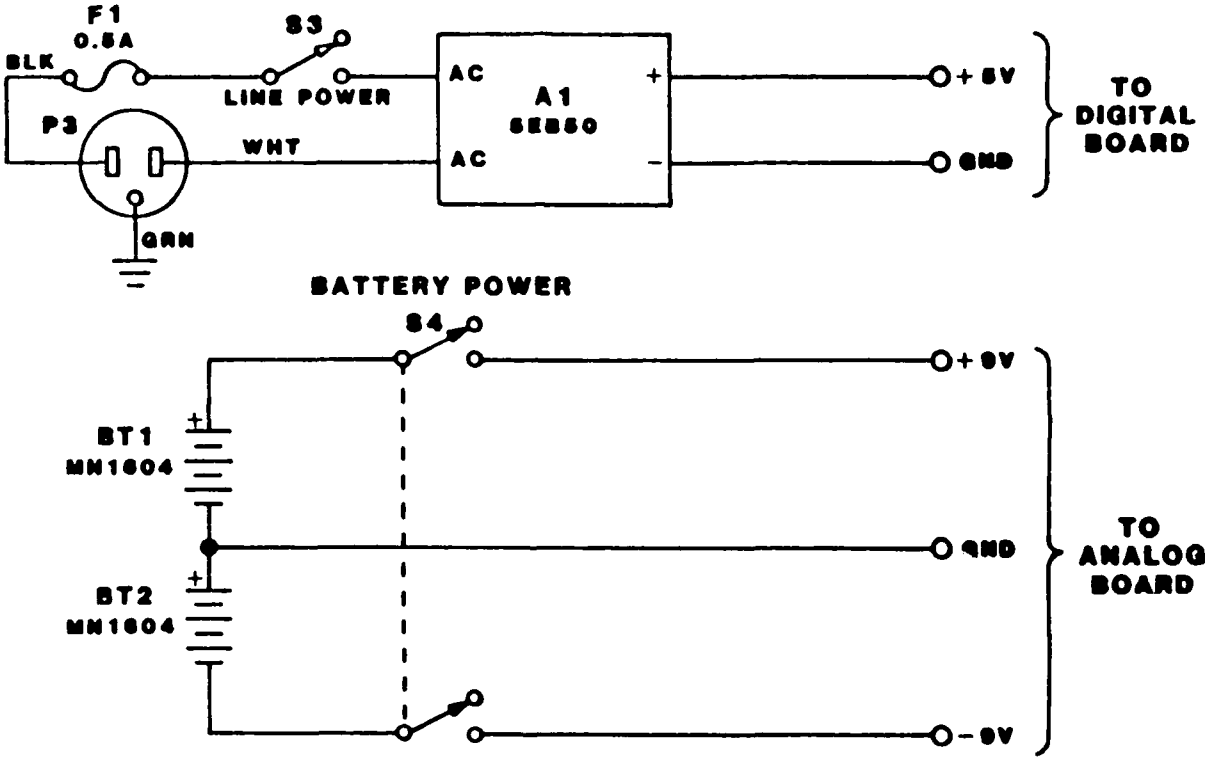

Figure 3. Schematic Diagram of Power Supplies

(7) Connect a jumper (e.g., a clip lead) between the two UNKNOWN terminals (i.e., the stiff wires projecting from the lefthand side of the cabinet).

(8) Adjust trimmer potentiometer R10 on the analog circuit board to produce a voltmeter reading of 0 V.

(9) Disconnect voltmeter from analog circuit board, move BATTERY POWER switch to the OFF position, and reinstall the front panel with four screws.

This completes the adjustment procedure.

2.3 Operating Procedures

2.3.1 Specimen Preparation

This instrument is designed to use a specimen of fuel-tank wall material approximately 3 in. square x 0.1 in. thick. Conductive electrodes must be applied to the weathered surface of the specimen to facilitate surface-resistance measurement; such electrodes are applied using a silver-conducting paint (e.g., GC Electronics catalog number 22-201 or equivalent) using a template to define the unpainted area. The template should be in the form of a circular annulus having an inside diameter of 2.50 in. and an outside diameter of 2.90 in. Template material can be thin paper, plastic or metal.

Center the template on the 3-in.-square specimen. Using a watercolor brush, apply a band of silver-conducting paint approximately 0.1 to 0.2 in. wide around the entire inner and outer peripheries of the template. Then, carefully lift the template away from the specimen; this should leave two circular electrodes with an unpainted annulus 0.20 in. wide between them. Allow the silver-conducting paint to dry according to manufacturer's recommendations before proceeding with surface-resistance measurement.

2.3.2 Measurement Procedure

(1) Place the specimen (electrode side up) on a sheet of high quality insulating material (e.g., Teflon, polystyrene, etc.) approximately 4 in. square and 0.063 in. thick.

(2) Place the specimen and its underlying insulator on the lefthand side of the instrument and arrange so that the two stiff wires projecting from the side of the instrument contact the two painted electrodes, one wire on each electrode.

(3) Move the RANGE switch to the lowest resistance range. If present, disconnect the jumper between UNKNOWN terminals.

(4) Connect the instrument line cord to a nominal 120-V, 60-Hz POWER source and move both the BATTERY POWER and the LINE POWER switches to their ON positions.

(5) Press the *READ* button and hold it depressed for 1 to 2 seconds; then release the button.

(6) When the digital display stabilizes and reads a fixed number, record the displayed number as representing specimen surface leakage resistance. If the display goes blank and the MSD decimal point illuminates, move the RANGE switch to the next highest resistance range and repeat the measurement procedure from Step (5) until a satisfactory reading is obtained. If it is not possible to obtain a good reading with the RANGE switch set to the highest resistance range, then it can be concluded that the specimen resistance is beyond the range of the instrument.

(7) When measurements are complete, return the RANGE switch to the lowest resistance range, connect a jumper (e.g., a clip lead) between the two stiff wires projecting from the lefthand side of the package, and move the BATTERY POWER and LINE POWER switches to their OFF positions.

3.0 Voltage-Divider

The voltage-divider instrument incorporates a range switch which facilitates selection of range resistors having values of 10^8 to 10^{13} ohms in decade steps. A zener diode provides the constant-voltage source necessary for supplying the voltage divider. A high-input-resistance electronic amplifier employing an MOS (metal-oxide-silicone) field-effect transistor or an electrometer tube as the input device transforms the voltage developed across the high-resistance UNKNOWN into an equivalent voltage available from a low-impedance source. Output of the electronic circuit is used to drive a standard d'Arsonval meter movement which is capable of displaying a two-decade range of resistance. Additionally, output of the electronic circuit is used to drive a guard band around all of the high-resistance components in the system. Also, this guard potential will be applied to the cable between the instrument cabinet and the probe. This cable is of triaxial configuration, that is, a single center conductor surrounded by two individually insulated coaxial shields. The outer shield is grounded, and the inner shield is connected to the guard circuit; this arrangement nulls the effects of stray leakages that are inherent in all insulating materials.

The instrument is battery powered from two standard 9-V transistor-radio batteries connected in series; thus, maximum voltage within the instrument is 18-V, and maximum potential applied across the UNKNOWN resistance (i.e., the fuel-tank specimen) is approximately 5-V. The instrument can be packaged in a metal case which can be grounded to eliminate static charge buildup.

Because resistance values encountered in insulation-resistance measurements are very high, even relatively low capacitances result in long charging time constants. Of course, as long as the circuit capacitance is charging, indicated value of resistance will be lower than the true resistance of the UNKNOWN specimen. If nothing is done about the charging problem, it could take as long as several minutes for each reading to allow the necessary charging to go to completion; however, in the proposed voltage-divider instrument, it is planned to incorporate a quick-charge feature that permits

making go/no-go measurements very quickly and absolute resistance measurements in much less time than would be possible without the quick-charge feature.

CAPACITANCE CHARGING INSTRUMENT
PARTS LIST, ANALOG BOARD

R1	Resistor, Composition, 10 kΩ	Allen Bradley	CB1035
R2	Resistor, Composition, 820 Ω	Allen Bradley	CB8215
R3	Resistor, Composition, 3.6 kΩ	Allen Bradley	CB3625
R4	Potentiometer, Trimming, 5.0 kΩ	Weston	860 W
R5	Resistor, Composition, 47 Ω	Allen Bradley	CB4705
R6	Resistor, Composition, 270 kΩ	Allen Bradley	CB2745
R7	Resistor, Composition, 270 kΩ	Allen Bradley	CB2745
R8	Resistor, Composition, 47 Ω	Allen Bradley	CB4705
R9	Resistor, Composition, 47 Ω	Allen Bradley	CB4705
R10	Potentiometer, Trimming, 2.0 kΩ	Weston	860 W
R11	Resistor, Composition, 4.7 kΩ	Allen Bradley	CB4725
R12	Resistor, Composition, 4.7 kΩ	Allen Bradley	CB4725
R13	Resistor, Composition, 4.7 kΩ	Allen Bradley	CB4725
R14	Resistor, Composition, 47 Ω	Allen Bradley	CB4705
R15	Resistor, Composition, 47 Ω	Allen Bradley	CB4705
R16	Resistor, Composition, 620 kΩ	Allen Bradley	CB6245
C1	Capacitor, Tantalum, 10 µF	Sprague 196D106X9050PE4	
C2	Capacitor, Mica, 10pF	Cornell-Dubilier CD10CC100J03	
C3	Capacitor, Mica, 100pF	Cornell-Dubilier CD10FC101J03	
C4	Capacitor, Mica, 10000pF	Cornell-Dubilier CD15FA102J03	
C5	Capacitor, Polycarbonate, 0.01 µF	TRW X440	
C6	Capacitor, Polycarbonate, 0.1 µF	TRW X440	
C7	Capacitor, Polycarbonate, 1.0 µF	TRW X463UW	
C8	Capacitor, Polycarbonate, 0.1 µF	TRW X440	
C9	Capacitor, Polycarbonate, 0.1 µF	TRW X440	
C10	Capacitor, Ceramic, 0.1 µF	Centralab CZ20A104M	
C11	Capacitor, Ceramic, 0.1 µF	Centralab CZ20A104M	
C12	Capacitor, Ceramic, 0.1 µF	Centralab CZ20A104M	
C13	Capacitor, Ceramic, 0.1 µF	Centralab CZ20A104M	
C14	Capacitor, Tantalum, 47 µF	Sprague 196D476X9020PE4	
C15	Capacitor, Tantalum, 47 µF	Sprague 196D476X9020PE4	
Q1	Transistor, MOSFET	Motorola 2N3769	
CR1	Diode, Zener	TRW LVA51	
U1	Integrated Circuit, Operational Amplifier	RCA CA3140S	
U2	Integrated Circuit, Voltage Comparator	National LM311N	
S1	Switch Section, Rotary	Centralab FFD	
	Switch, Index Assembly	Centralab P-271	
S2	Switch, Pushbutton	Alcoswitch TPF21RG-RA(O)	
	Printed-Circuit Board, Analog	SwRI	
	Bracket, Switch	SwRI	
	Push Rod	SwRI	
	Bushing	H.H. Smith 184	
	Knob	Kurz-Kasch S-647-3L	

PARTS LIST, ANALOG BOARD (Continued)

Terminal	Useco	2000B
Terminal	Useco	2030B
Miscellaneous Hardware		

PARTS LIST, DIGITAL BOARD (Continued)

R21	Resistor, Composition, 1.0 kΩ	Allen Bradley CB1025
R22	Resistor, Composition, 110 kΩ	Allen Bradley CB1145
R23	Resistor, Composition, 15 kΩ	Allen Bradley CB1535
R24	Resistor, Composition, 1.0 kΩ	Allen Bradley CB1025
R25	Resistor, Composition, 1.0 kΩ	Allen Bradley CB1025
R26	Resistor, Composition, 1.0 kΩ	Allen Bradley CB1025
R27	Resistor, Composition, 1.0 kΩ	Allen Bradley CB1025
R28	Resistor, Composition, 1.0 kΩ	Allen Bradley CB1025
R29	Resistor, Composition, 1.0 kΩ	Allen Bradley CB1025
R30	Resistor, Composition, 1.0 kΩ	Allen Bradley CB1025
R31	Resistor, Composition, 1.0 kΩ	Allen Bradley CB1025
R32	Resistor, Composition, 1.0 kΩ	Allen Bradley CB1025
R33	Resistor, Composition, 1.0 kΩ	Allen Bradley CB1025
R34	Resistor, Composition, 1.0 kΩ	Allen Bradley CB1025
R35	Resistor, Composition, 1.0 kΩ	Allen Bradley CB1025
R36	Resistor, Composition, 1.0 kΩ	Allen Bradley CB1025
R37	Resistor, Composition, 200 Ω	Allen Bradley CB2015
R38	Resistor, Composition, 200 Ω	Allen Bradley CBB015
R39	Resistor, Composition, 200 Ω	Allen Bradley CB2015
R40	Resistor, Composition, 200 Ω	Allen Bradley CB2015
R41	Resistor, Composition, 200 Ω	Allen Bradley CB2015
R42	Resistor, Composition, 200 Ω	Allen Bradley CB2015
R43	Resistor, Composition, 200 Ω	Allen Bradley CB2015
R44	Resistor, Composition, 200 Ω	Allen Bradley CB2015
R45	Resistor, Composition, 200 Ω	Allen Bradley CB2015
R46	Resistor, Composition, 200 Ω	Allen Bradley CB2015
R47	Resistor, Composition, 200 Ω	Allen Bradley CB2015
R48	Resistor, Composition, 200 Ω	Allen Bradley CB2015
R49	Resistor, Composition, 200 Ω	Allen Bradley CB2015
R50	Resistor, Composition, 200 Ω	Allen Bradley CB2015
R51	Resistor, Composition, 200 Ω	Allen Bradley CB2015
R52	Resistor, Composition, 200 Ω	Allen Bradley CB2015
R53	Resistor, Composition, 200 Ω	Allen Bradley CB2015
R54	Resistor, Composition, 200 Ω	Allen Bradley CB2015
R55	Resistor, Composition, 200 Ω	Allen Bradley CB2015
R56	Resistor, Composition, 200 Ω	Allen Bradley CB2015
R57	Resistor, Composition, 200 Ω	Allen Bradley CB2015
R58	Resistor, Composition, 200 Ω	Allen Bradley CB2015
R59	Resistor, Composition, 200 Ω	Allen Bradley CB2015
R60	Resistor, Composition, 200 Ω	Allen Bradley CB2015
R61	Resistor, Composition, 200 Ω	Allen Bradley CB2015
R62	Resistor, Composition, 200 Ω	Allen Bradley CB2015
R63	Resistor, Composition, 200 Ω	Allen Bradley CB2015

PARTS LIST, DIGITAL BOARD (Continued)

R64	Resistor, Composition, 200 Ω	Allen Bradley CB2015
R65	Resistor, Composition, 200 Ω	Allen Bradley CB2015
C21	Capacitor, Ceramic, 0.1 μF	Centralab CZ20A104M
C22	Capacitor, Ceramic, 0.01 μF	Centralab CZ15C103M
C23	Capacitor, Polycarbonate, 0.1 μF	TRW X440
C24	Capacitor, Ceramic, 0.1 μF	Centralab CZ20A104M
C25	Capacitor, Ceramic, 0.1 μF	Centralab CZ20A104M
C26	Capacitor, Ceramic, 0.1 μF	Centralab CZ20A104M
C27	Capacitor, Ceramic, 0.1 μF	Centralab CZ20A104M
C28	Capacitor, Ceramic, 0.1 μF	Centralab CZ20A104M
C29	Capacitor, Ceramic, 0.1 μF	Centralab CZ20A104M
C30	Capacitor, Ceramic, 0.1 μF	Centralab CZ20A104M
C31	Capacitor, Ceramic, 0.1 μF	Centralab CZ20A104M
C32	Capacitor, Ceramic, 0.1 μF	Centralab CZ20A104M
C33	Capacitor, Ceramic, 0.1 μF	Centralab CZ20A104M
C34	Capacitor, Ceramic, 0.1 μF	Centralab CZ20A104M
C35	Capacitor, Ceramic, 0.1 μF	Centralab CZ20A104M
C36	Capacitor, Tantalum, 47 μF	Sprague 196D476X9020PE4
U21	Integrated Circuit, Timer	National LM555CN
U22	Integrated Circuit, Dual 4-Input NAND	Texas Instruments SN7420N
U23	Integrated Circuit, Quad 2-Input NAND	National DM7400N
U24	Integrated Circuit, Decade Counter	National DM7490N
U25	Integrated Circuit, Decade Counter	National DM7490N
U26	Integrated Circuit, Decade Counter	National DM7490N
U27	Integrated Circuit, Decade Counter	National DM7490N
U28	Integrated Circuit, BCD/7-Seg. Decoder	Texas Instruments SN7446AN
U29	Integrated Circuit, BCD/7-Seg. Decoder	Texas Instruments SN7446AN
U30	Integrated Circuit, BCD/7-Seg. Decoder	Texas Instruments SN7446AN
U31	Integrated Circuit, BCD/7-Seg. Decoder	Texas Instruments SN7446AN
U32	Integrated Circuit, Dual Type-D Flip-Flop	Signetics 74S74N
U33	Integrated Circuit, Hex Inverting Buffer	Texas Instruments SN7406N
U34	Display, 7-Segment	Litronix 707
U35	Display, 7-Segment	Litronix 707
U36	Display, 7-Segment	Litronix 707
U37	Display, 7-Segment	Litronix 707
S2	(See Analog Board Parts List)	
J1	Connector, PC Mount	T&B/Ansley 609-3414
J2	Connector, PC Mount	T&B/Ansley 609-3414
P1	Connector, Cable	T&B/Ansley 609-3430
	Strain Relief	T&B/Ansley 609-3431
P2	Connector, Cable	T&B/Ansley 609-3430
	Strain Relief	T&B Ansley 609-3431
	Printed-Circuit Board, Digital	SwRI
	Printed-Circuit Board, Display	SwRI
	Socket, Integrated Circuit	Augat 516-AG11D

PARTS LIST, DIGITAL BOARD (Continued)

	Component Carrier	Augat 616-CG1
	Pin, Wire-Wrap	Augat 314-17P2
	Terminal	Useco 2000B
	Miscellaneous Hardware	--
A1	POWER Supply, 5V	Acopian 5EB50
S1	(See Analog Board Parts List)	
S2	(See Analog Board Parts List)	
S3	Switch, Toggle	Alcoswitch MTA206N
S4	Switch, Toggle	Alcoswitch MTA206N
F1	Fuse, 0.5A	Littelfuse 3AG
	Fuse Holder	Littelfuse 342022A
BT1	Battery, 9V Alkaline	Mallory MN1604
BT2	Batrery, 9V Alkaline	Mallory MN1604
P3	Line Cord, 3-Wire	Belden 17237
	Cabinet	Bud SB-2140
	Miscellaneous Hardware	--

DISTRIBUTION LIST

DEPARTMENT OF DEFENSE

DEFENSE SYSTEMS MANAGEMENT COLLEGE 1
OFFICE OF THE COMMANDANT
FORT BELVOIR VA 22060-5191

DEFENSE DOCUMENTATION CTR
CAMERON STATION 12
ALEXANDRIA VA 22314

DEPT. OF DEFENSE
ATTN: OASD (A&L) (MR DYCKMAN) 1
WASHINGTON DC 20301-8000

DEFENSE ADVANCED RES PROJ AGENCY
DEFENSE SCIENCES OFC 1
1400 WILSON BLVD
ARLINGTON VA 22209

DEPARTMENT OF THE ARMY

CDR
U.S. ARMY BELVOIR RESEARCH, DEVELOPMENT & ENGINEERING CTR
ATTN: STRBE-VF 10
STRBE-VU 10
STRBE-WC 2
FORT BELVOIR VA 22060-5606

CDR
US ARMY MATERIEL DEVEL & READINESS COMMAND
ATTN: AMCLD (DR ODOM) 1
AMCDE-SG 1
AMCDE-SS 1
AMCQA-E 1
AMCSM-WST (LTC DACEY) 1
AMCIP-P (MR HARVEY) 1
5001 EISENHOWER AVE
ALEXANDRIA VA 22333-0001

CDR
US ARMY TANK-AUTOMOTIVE CMD
ATTN: AMSTA-RG (MR WHEELOCK) 1
AMSTA-TSL (MR BURG) 1
AMSTA-G 1
AMSTA-MTC (MR GAGLIO), AMSTA-MC, AMSTA-MV 1
AMSTA-UBP (MR MCCARTNEY) 1
AMSTA-MLF (MR KELLER) 1
WARREN MI 48397-5000

DIRECTOR
US ARMY MATERIEL SYSTEMS ANALYSIS ACTIVITY
ATTN: AMXSY-CM (MR NIEMEYER) 1
AMXSY-CR 1
ABERDEEN PROVING GROUND MD
21005-5006

DIRECTOR
APPLIED TECHNOLOGY LAB
U.S. ARMY R&T LAB (AVSCOM)
ATTN: SAVDL-ATL-ATP (MR MORROW) 1
SAVDL-ATL-ASV 1
FORT EUSTIS VA 23604-5577

CDR
US ARMY COLD REGION TEST CENTER
ATTN: STECR-TA 1
APO SEATTLE 98733

HQ, DEPT. OF ARMY
ATTN: DAEN-DRM 1
WASHINGTON DC 20310

CDR
US ARMY ABERDEEN PROVING GROUND
ATTN: STEAP-MT-U (MR DEAVER) 1
ABERDEEN PROVING GROUND MD
21005

CDR
US ARMY YUMA PROVING GROUND
ATTN: STEYP-MT-TL-M (MR DOEBBLER) 1
YUMA AZ 85364-9130

CDR
US ARMY RESEARCH OFC
ATTN: SLCRO-ZC 1
SLCRO-EG (DR MANN) 1
SLCRO-CB (DR GHIRARDELLI) 1
P O BOX 12211
RSCH TRIANGLE PARK NC 27709-2211

DIR
US ARMY AVIATION R&T LAB (AVSCOM)
ATTN: SAVDL-AS (MR WILSTEAD) 1
AMES RSCH CTR
MAIL STOP 207-5
MOFFET FIELD CA 94035

CDR
US ARMY ORDNANCE CENTER & SCHOOL
ATTN: ATSL-CD-CS 1
ABERDEEN PROVING GROUND MD 21005

CDR, US ARMY TROOP SUPPORT COMMAND
ATTN: AMSTR-ME 1
AMSTR-S 1
4300 GOODFELLOW BLVD
ST LOUIS MO 63120-1798

TRADOC LIAISON OFFICE
ATTN: ATFE-LO-AV 1
4300 GOODFELLOW BLVD
ST LOUIS MO 63120-1798

HQ
US ARMY TRAINING & DOCTRINE CMD
ATTN: ATCD-SL-5 (MAJ JONES) 1
FORT MONROE VA 23651-5000

DIRECTOR
US ARMY RSCH & TECH LAB (AVSCOM)
PROPULSION LABORATORY
ATTN: SAVDL-PL-D (MR ACURIO) 1
21000 BROOKPARK ROAD
CLEVELAND OH 44135-3127

CDR
US ARMY NATICK RES & DEV LAB
ATTN: STRNA-YE (DR KAPLAN) 1
STRNA-U 1
NATICK MA 01760-5000

CDR
US ARMY QUARTERMASTER SCHOOL
ATTN: ATSM-CD 1
ATSM-TD 1
ATSM-PFS 1
FORT LEE VA 23801

DIR
US ARMY MATERIALS & MECHANICS RESEARCH CENTER
ATTN: SLCMT-M 1
SLCMT-O 1
WATERTOWN MA 02172-2796

DEPARTMENT OF THE NAVY

CDR
NAVAL AIR PROPULSION CENTER
ATTN: PE-33 (MR D'ORAZIO) 1
PE-32 (MR MANGIONE) 1
P O BOX 7176
TRENTON NJ 06828

CDR
NAVAL SEA SYSTEMS CMD
ATTN: CODE 05M4 (MR R LAYNE) 1
WASHINGTON DC 20362-5101

CDR
DAVID TAYLOR NAVAL SHIP R&D CTR
ATTN: CODE 2830 (MR BOSMAJIAN) 1
CODE 2759 (MR STRUCKO) 1
CODE 2831 1
ANNAPOLIS MD 21402

CDR
NAVAL AIR DEVELOPMENT CTR
ATTN: CODE 60612 1
WARMINSTER PA 18974

CDR
NAVAL RESEARCH LABORATORY
ATTN: CODE 6170 1
CODE 6180 1
CODE 6110 (DR HARVEY) 1
WASHINGTON DC 20375

COMMANDING GENERAL
US MARINE CORPS DEVELOPMENT & EDUCATION COMMAND
ATTN: DO74 (LTC WOODHEAD) 1
QUANTICO VA 22134

OFFICE OF THE CHIEF OF NAVAL RESEARCH
ATTN: OCNR-126 (MR ZIEM) 1
ARLINGTON, VA 22217-5000

CDR
NAVY PETROLEUM OFC
ATTN: CODE 43 (MR LONG) 1
CAMERON STATION
ALEXANDRIA VA 22304-6180

DEPARTMENT OF THE AIR FORCE

CDR
US AIR FORCE WRIGHT AERONAUTICAL LAB
ATTN: AFWAL/POSF (MR CHURCHILL) 1
AFWAL/POSL (MR JONES) 1
AFWAL/MLSE (MR MORRIS) 1
AFWAL/MLBT (MR SNYDER) 1
WRIGHT-PATTERSON AFB OH 45433

CDR
SAN ANTONIO AIR LOGISTICS CTR
ATTN: SAALC/SFT (MR MAKRIS) 1
SAALC/MMPRR 1
KELLY AIR FORCE BASE TX 78241

CDR
WARNER ROBINS AIR LOGISTIC CTR
ATTN: WRALC/MMTV (MR GRAHAM) 1
ROBINS AFB GA 31098

OTHER GOVERNMENT AGENCIES

NATIONAL AERONAUTICS AND SPACE ADMINISTRATION
VEHICLE SYSTEMS AND ALTERNATE FUELS PROJECT OFFICE
ATTN: MR CLARK 1
LEWIS RESEARCH CENTER
CLEVELAND OH 44135

DEPARTMENT OF TRANSPORTATION
FEDERAL AVIATION ADMINISTRATION
ATTN: AWS-110 1
800 INDEPENDENCE AVE, SW
WASHINGTON DC 20590

US DEPARTMENT OF ENERGY
CE-151
ATTN: MR ECKLUND 1
FORRESTAL BLDG.
1000 INDEPENDENCE AVE, SW
WASHINGTON DC 20585

ENVIRONMENTAL PROTECTION AGENCY
AIR POLLUTION CONTROL 1
2565 PLYMOUTH ROAD
ANN ARBOR MI 48105

AGENCY FOR INTERNATIONAL DEVELOPMENT
ATTN: MR D HOOKER 1
M/SER/EOMS/OPM, ROOM 2155A11
WASHINGTON, DC 20523

END

DTIC

5-86